



A Review of Advances in Triaxial Tests: Instruments, Test Techniques and Prospects

Jitao Bai^a, Yu Diao^a, Chenhong Jia^a, Chongyang Liu^a, Menghan Zhang^a, and Chu Wang^a

^aDept. of Civil Engineering, Key Laboratory of Coast Civil Structures and Safety of Ministry of Education, Tianjin University, Tianjin 300072, China

ARTICLE HISTORY

Received 29 July 2021
Revised 16 January 2022
Accepted 28 February 2022
Published Online 28 June 2022

KEYWORDS

Triaxial tests
Geotechnical engineering
Instruments
Test techniques
Prospects

ABSTRACT

Triaxial test is approved to be the most suitable method for studying the mechanical properties of rocks and soils in lab. Through conventional triaxial tests, parameters like the strength of rocks and soils can be obtained, thus providing guidance for the design and construction of geotechnical engineering. With the development of geotechnical engineering, more and more new problems that can hardly be solved by conventional triaxial tests have arisen, which can be classified into two categories: one is the mechanical properties of special soils (rocks), and the other is the mechanical properties of the soils (rocks) under special conditions like geologic hazards and multi-field coupling. The paper introduced several new types of triaxial instruments and test techniques developed in response to the problems, and prospects have been made for further study of triaxial tests, which may provide reference for the optimization of triaxial tests.

1. Introduction

Triaxial tests are considered to be the most effective way to study the mechanical properties of rocks and soils (Yang et al., 2018). According to the stress state during the test, triaxial tests can be divided into conventional triaxial tests (stress state: $\sigma_1 > \sigma_2 = \sigma_3 > 0$) and true triaxial tests (stress state: $\sigma_1 > \sigma_2 > \sigma_3 > 0$) (Liu and Tang, 2008). Conventional triaxial tests are relatively simple both in instruments and operation and is more commonly used in practical engineering. While true triaxial tests are relatively complicated, which is generally used for laboratory research or special projects that are rather complex.

Conventional triaxial apparatus is mainly composed of three parts: axial loading equipment, lateral loading equipment and pressure chamber. During the test, sample wrapped with rubber membrane is placed in the pressure chamber and the predetermined confining pressure σ_3 is first applied and kept unchanged. Then the axial load is increased at a certain rate until the sample is damaged. By changing the confining pressure and other parameters, various geomechanical indexes such as triaxial compression strength, strength envelope and shear strength parameters (c , φ) under different confining pressures can be obtained, thereby

providing guidance for geotechnical engineering. However, there are two principal stresses that are always equal in conventional triaxial tests, while natural rocks and soils are usually in a complex three-dimensional stress state where the three principal stresses are unequal to each other. Therefore, the results obtained by conventional triaxial tests cannot completely reflect the real conditions.

Compared with conventional triaxial tests, true triaxial tests can realize independent control of three-dimensional stress and the test results are much closer to the real conditions. True triaxial apparatus was first developed by Kjellman (1936) in 1936. In the following century, people have developed varieties of true triaxial apparatuses. Currently, true triaxial apparatuses can be classified into three main categories based on different boundaries (Yin et al., 2010; Wang, 2018):

1. True triaxial apparatus with rigid boundaries (Hambly, 1969; Wood, 1974; Ibsen and Praastrup, 2002; Ismail et al., 2005; Sun et al., 2008). The three principal stresses are applied by six rigid plates in three orthogonal directions.
2. True triaxial apparatus with flexible boundaries (Bell, 1965; Choi et al., 2008; Voznesensky et al., 2013). The three principal stresses are applied by six flexible bladders (usually flexible

CORRESPONDENCE Yu Diao ✉ yudiao@tju.edu.cn ☒ Dept. of Civil Engineering, Key Laboratory of Coast Civil Structures and Safety of Ministry of Education, Tianjin University, Tianjin 300072, China

membranes with liquid pressure inside) in three orthogonal directions.

3. True triaxial apparatus with mixed rigid and flexible boundaries (Green, 1969; Hoyos and Macari, 2001; Yin et al., 2010; Yin et al., 2011; Hoyos et al., 2012; Shao et al., 2017; Zheng et al., 2020; Zheng et al., 2021). The three principal stresses are applied by a mixture of rigid plates and flexible membrane faces in three orthogonal directions.

True triaxial apparatus can effectively simulate the complex stress state of rocks and soils. But in general, current tests carried out on true triaxial apparatus are still relatively simple.

With the development of geotechnical engineering, many new problems encountered in practical engineering need to be solved urgently. These problems can be classified into two categories: one is the mechanical properties of special soils (rocks), and the other is the mechanical properties of the soils (rocks) under special conditions like geologic hazards and multi-field coupling. Therefore, it is necessary to improve the triaxial apparatuses and introduce more advanced test techniques to meet the test conditions required by the study of those problems. In this paper, several new triaxial test instruments and related test techniques are introduced, and prospects are made for further study of triaxial tests based on the characteristics of the current study on triaxial test instruments and test techniques, which is expected to provide reference for the optimization of triaxial tests.

2. Triaxial Test Apparatus

2.1 Triaxial Apparatus for Special Soils

2.1.1 Triaxial Test System for Hydrate Sediments

Natural gas hydrate, commonly known as “combustible ice”, is a solid crystal formed by methane molecules trapped in a cage of water molecules under low temperature and high-pressure conditions. As a new energy source with high calorific value and low environmental pollution, natural gas hydrate has attracted much attention in recent years. Like other mineral resources, the mining of natural gas hydrates also requires the support of geomechanical tests. However, because of engineering challenges, coring and in-situ testing are still difficult to achieve (Yoneda et al., 2019). Meanwhile, since the deformation behavior and change in shear strength of hydrate sediments haven’t been clearly understood, its mechanical modeling is still challenging (Li et al., 2019b). Different models may adopt different parameters or conditions, thus leading to different conclusions. Therefore, the indoor triaxial test is believed to be an accessible and effective method at present. Researchers (Miyazaki et al., 2011; Hyodo et al., 2013; Choi et al., 2018; Zhang et al., 2018; Li et al., 2019a; Dong et al., 2020; Nakashima et al., 2021; Wang et al., 2021a) have made various improvements on triaxial test instruments to make them suitable for triaxial shear tests of hydrate sediments under different conditions, and the influence of factors like soil types, confining pressure, pore pressure and hydrate saturation on the strength and deformation properties of hydrate sediments

have been investigated. However, the problems of effective confining pressure control, strain measurement and the decomposition of hydrate sediments in triaxial tests have not been well resolved.

Actually, the effective confining pressure control during the formation of hydrate, the measurement of sample strain during loading and the control of decomposition process are three main problems arise in triaxial tests for hydrate sediments. The formation of hydrate usually starts by injecting a certain amount of gas into the sediment specimen placed in pressure chamber. As the hydration reaction going on, the air pressure in the sample will gradually decrease due to the consumption of gas. If the confining pressure maintains unchanged during the process, the effective confining pressure will increase, causing the sample to be in a loaded state before triaxial loading and eventually affect the final test results. Therefore, it is necessary to achieve real-time adjustment of confining pressure for triaxial apparatus to keep the effective confining pressure constant. In addition, since the decomposition of the hydrate can significantly affect the mechanical properties of hydrate sediments and the deformation properties of the sample under different loads are essential for the establishment of the constitutive model, it is also necessary for triaxial apparatus to obtain the strain of the sample (including the axial strain and the radial strain/volumetric strain) and have the ability to control the hydrate decomposition. In this regard, Zhou et al. (2020a) developed a multi-functional triaxial test system for hydrate sediments that can realize the functions of tracking confining pressure changes, measuring volumetric strain and controlling hydrate decomposition. As shown in Fig. 1, the testing system is composed of a supply-exhaust module, a stress loading module, a temperature control module, a data acquisition module and an auxiliary module.

In the supply-exhaust module, the high-pressure gas cylinder G1 provides the gas source, and the buffer container G2 stores the gas. The gas can enter the pressure chamber through the pipe and interact with the water in sample G3 to form hydrate. The return-pump G4 controls the upper limit of the air pressure. When the pressure of the return-pump is greater than the air

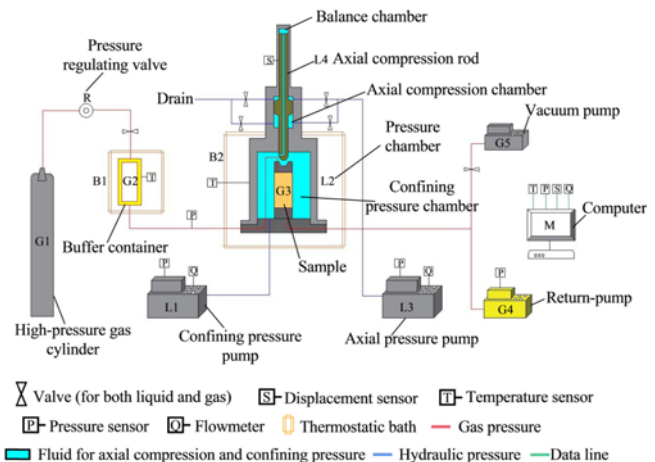


Fig. 1. Schematic Diagram of Triaxial Test System for Hydrate Bearing Sediment (after Zhou et al., 2020a)

pressure, the gas cannot pass through, otherwise it can be discharged through the return-pump. The vacuum pump G5 can pump out the impurities in the buffer container, sample and pipeline. In the stress loading module, the confining pressure pump L1 provides confining pressure through liquid, the pressure chamber L2 provides space for hydrate synthesis and triaxial shear, the axial pressure pump L3 applies axial pressure through the liquid, and the axial compression rod L4 transmits axial pressure to the sample. In addition, the system can also control the temperature of the buffer container through the thermostatic bath B1 and that of the pressure chamber and the sample through the thermostatic bath B2.

2.1.2 Triaxial Apparatus for Unsaturated Soils

Compared with saturated soils, unsaturated soils mainly have two features. First, unsaturated soils have multiple phases in composition. In addition to the well-known three phases of solid, liquid and gas, the boundary between liquid and gas (namely a free surface) is not to be regarded as a simple geometrical plane, but rather as a membrane of a certain thickness, which is believed to behave as if in a tensile stress state (Davies and Rideal, 1963). The second is that, in unsaturated soils, the material variables generally vary with the state variables (Lu and Likos, 2004). Therefore, unsaturated soils are quite different from saturated soils in mechanical properties, and unsaturated soil mechanics has been the focus of geotechnical engineering in recent years. Usually, modern triaxial tests for unsaturated soils should accommodate the independent measurement and control of pore air pressure, pore water pressure and volume changes (Wulfsohn et al., 1998). Besides, the control of three-dimensional stress, temperature and humidity as well as the permeability measurement are also considered in unsaturated soil triaxial tests.

2.1.2.1 Measurement of Volume Changes

Volume changes of unsaturated soils in triaxial tests can usually be measured through the volume changes of the water in triaxial cell, the volume changes of the fluid in the sample, and the strain of the sample.

Ng et al. (2002) proposed a new total volume measuring triaxial apparatus for unsaturated soils, as shown in Fig. 2. The overall volume change of the specimen is obtained by recording the differential pressures between the water inside the inner chamber and the water inside a reference tube through a high-accuracy differential pressure transducer (DPT). Essentially, the volume changes of the specimen in this apparatus are measured by the volume changes of the water in inner chamber, and it is the volume changes of the water in inner chamber that leads to differential water pressures. There are some advantages of the apparatus.

1. The inner chamber is designed to be open-ended and bottle-shaped, which has a neck with the inner diameter slightly larger than that of the loading ram. This means that even a small volume change in the specimen can lead to an obvious change in the water level of the inner chamber, thus endow the apparatus with much higher accuracy and

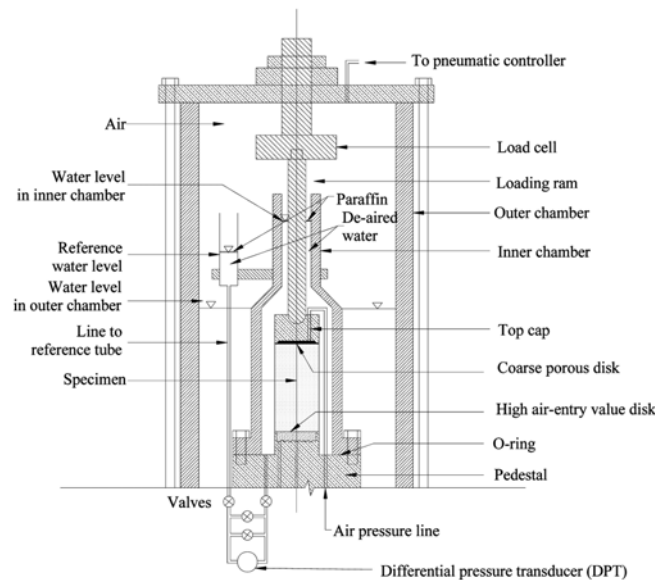


Fig. 2. Total Volume Measuring Triaxial Apparatus for Unsaturated Soils (after Ng et al., 2002)

sensitivity. Besides, the adoption of the high-accuracy DPT also guaranteed the accuracy of the measurement.

2. The open-ended design at the top of the inner chamber ensures the same pressure both inside and outside the inner chamber, thus eliminating the deformation of the inner chamber caused by pressure differences.
3. As for the materials, the wall of the inner chamber is made of aluminum, which is generally believed to have relatively negligible creep and hysteretic effects and lower water absorption. Besides, bronze is adopted for connecting tubes to minimize the potential expansion or compression.

The second method to measure the volume changes of the sample is based on the volume changes of pore water and pore air. Wulfsohn et al. (1998) introduced a triaxial system composed of a cabinet mounted triaxial chamber, a digital pressure-volume controller, plumbing arrangements, data acquisition system and host computer. The triaxial chamber is specially modified so that it can be applied to unsaturated soil tests, control the pore air pressure and measure the pore water pressure as well as the volume changes of pore water and pore air respectively.

As is shown in Fig. 3, the measurement for volume changes of pore water is conducted through port *a*, pore-water pressure is measured by a pressure transducer through port *b*, pore air pressure control and volume change measurements are conducted through port *c* by a digital pressure-volume controller, and a constant chamber pressure is supplied by a compressor through port *d*. During the tests, the axial force and axial displacement are applied from the base of the chamber through a screw-driven actuator, and can be respectively measured through a submersible load cell located at the top of the chamber and an axial actuator encoder with a resolution of 0.2 μm . Since a balanced ram has been applied to the system, which can keep the chamber pressure constant under high-speed movement, the system is also capable

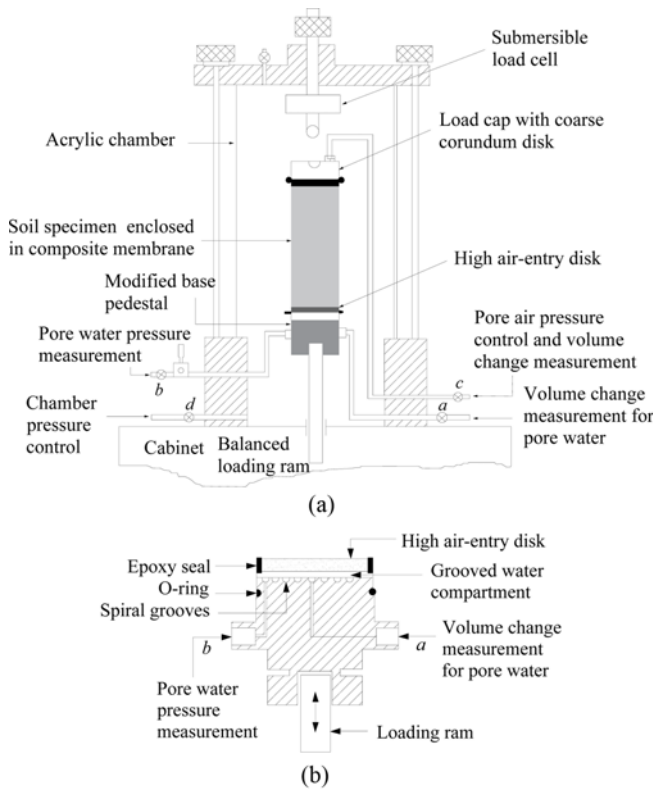


Fig. 3. Triaxial Chamber for Unsaturated Soil Testing (after Wulfsohn et al., 1998): (a) Triaxial Chamber, (b) Modified Base Pedestal

of dynamic cyclic tests.

The volume changes can also be obtained from the strain of the sample. Usually, axial and lateral strains are measured in triaxial tests, and then the volume changes of the sample can be calculated. Desrues et al. (1996) reported a study of strain localization in triaxial tests on sand through X-ray computed tomography (X-ray CT). Garga and Zhang (1997) developed a Hall effect radial displacement transducer (HRDT). With the aid of the HRDT and the linear variable differential transformer (LVDT), the volume change of the sample during triaxial tests can be easily obtained. Rampino et al. (1999) introduced a new stress-path chamber for unsaturated soils, in which the volume changes of the sample are obtained by measuring axial strains and radial strains separately.

In recent years, some new techniques have been adopted in volume change measurement. Zhang et al. (2014b) introduced a novel laser sensor volume measurement system, which can achieve continuous volume measurements up to large strain levels during triaxial tests for unsaturated soils, including the post-peak region of the brittle, artificially cemented specimens that cannot be reliably measured by local measurement techniques like LVDTs and Hall effect sensors. Li et al. (2016) addressed in-depth discussions on the photogrammetry-based method used for total and localized volume change measurements on unsaturated soils during triaxial tests, including system setup, the measurement procedure, accuracy self-check and data post-processing. Uzun and Korsunsky (2019) introduced the height digital image correlation

(hDIC) technique for the identification of triaxial deformations. Those new techniques provide researchers with more choices in measuring the volume change conveniently.

2.1.2.2 Measurement and Control of Pore Pressure

Pore water pressure and pore air pressure are important in unsaturated soil mechanics. In triaxial tests for unsaturated soils, negative pore water pressure can be directly measured by tensiometers (in the lab and the field) and the axis-translation apparatus (only in the lab) (Fredlund and Rahardjo, 1993), while pore air pressure can be controlled or measured by digital pressure controller (Wulfsohn et al., 1998) or pressure transducer (Ishikawa et al., 2014). Besides, osmotic technique can also be used to control pore water pressure.

Cui and Delage (1996) designed an osmotic triaxial apparatus as shown in Fig. 4, and the pore water pressure is controlled by osmotic technique. The apparatus is mainly composed of an inner chamber, an outer chamber and a solution circulation system, and the inner chamber and the outer chamber is connected. In the solution circulation system, the solution of polyethylene glycol with the molecular weight of 15,000 – 20,000 (PEG 20000) is pumped from the reservoir to the top cap of the inner chamber, then go through the base of the inner chamber and finally back to the reservoir. The sample is put in the inner chamber in contact on both bottom and top surfaces with the semi-permeable membranes, through which an osmotic suction is applied to the sample by the circulated solution of PEG 20000 and thus resulting in negative pore water pressure within the sample. At the bottom of the inner chamber, an air vent is machined to ensure a constant pore air pressure equal to atmospheric pressure in the sample. The inner chamber is filled with slightly colored water around the sample with a thin layer of silicon oil on it, and a cathetometer is adopted to monitor the volume changes based on the changes of the oil-air interface level.

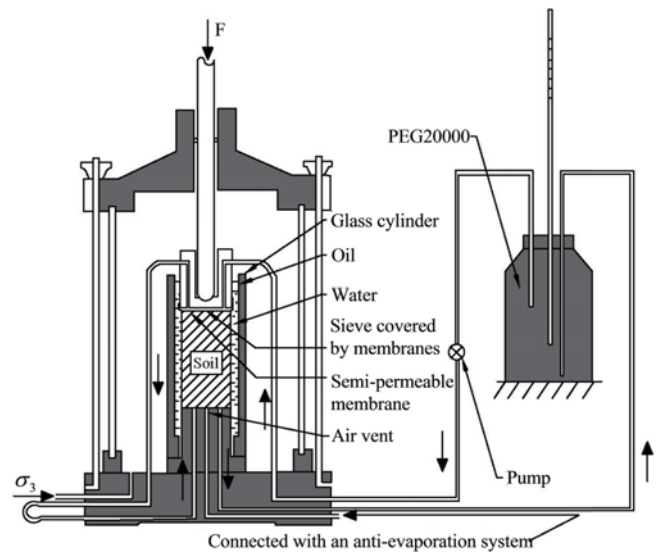


Fig. 4. Osmotically Controlled Suction Triaxial Apparatus (after Cui and Delage, 1996)

2.1.2.3 Control of Three-Dimensional Stress

Like saturated soils, triaxial tests for unsaturated soils can also be conducted under different conditions, including three-dimensional stress, thermo-mechanical coupling, permeability and multiple cycles of drying and wetting.

Three-dimensional stress conditions are usually achieved by true triaxial apparatus. Matsuoka et al. (2002) developed a rigid loading true triaxial apparatus that can realize suction control for unsaturated soils. Hoyos et al. (2012) introduced a hybrid loading true triaxial apparatus with flexible boundaries, which can also realize suction control and has a wide range of stress paths. Zheng et al. (2020) introduced a new suction-controlled true triaxial apparatus with mixed rigid-flexible boundaries, shown as Fig. 5. During the tests, forces are imposed on specimens in three orthogonal directions via three independent servo-driven hydraulic systems and are measured by hydraulic transducers. The vertical forces are provided by the piston at the axial bottom of the pressure chamber (rigid) and the lateral ones by hydraulic rubber bags (flexible). The pore air pressure is provided and regulated by the water/air control system, and is separated from the pore water pressure that is measured by the pore water pressure transducer. As for displacement measurement, it is realized through displacement transducers set in three directions.

2.1.2.4 Temperature Control

To study the properties of unsaturated soils under different temperatures, Cai et al. (2014) presented a triaxial apparatus with a temperature and a suction control system. The temperature-

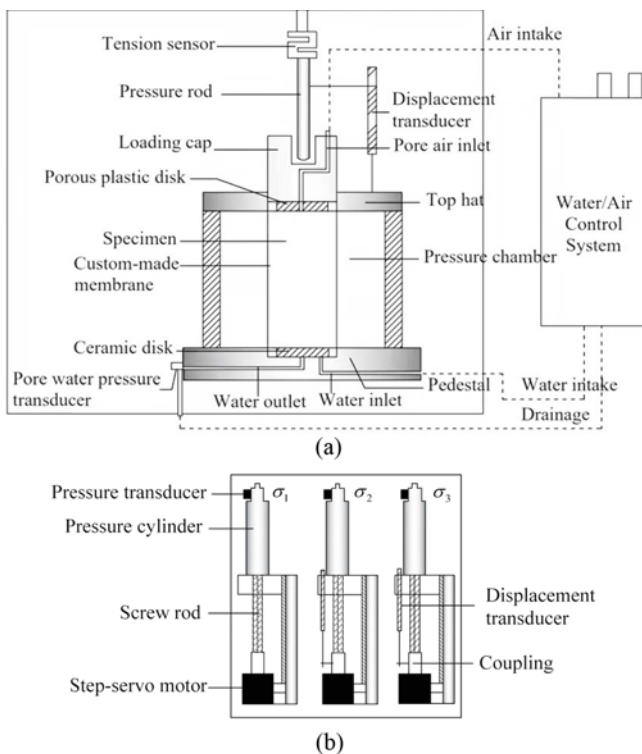


Fig. 5. Suction-Controlled True Triaxial Apparatus with Rigid-Flexible Boundaries (after Zheng et al., 2020)

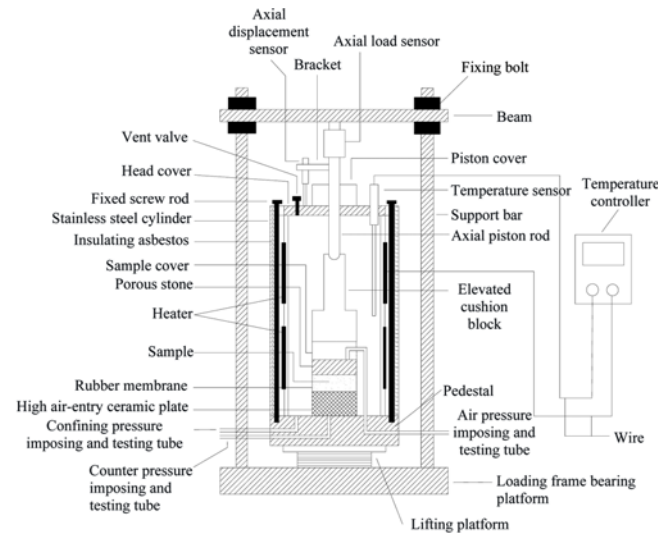


Fig. 6. Temperature-Controlled Pressure Chamber in Triaxial Apparatus for Unsaturated Soils (after Cai et al., 2014)

controlled pressure chamber, which is the key part of the apparatus, as shown in Fig. 6. Heating of the sample is achieved indirectly by heating the water in the chamber so that the sample can be heated evenly. Once the target temperature has been set during the test, the temperature controller will order the heater to be working until the feedback from the temperature sensor indicates the target temperature has been reached. When the temperature falls as a consequence of heat loss, the heater will start to work again to maintain the temperature at the desired value. To reduce the heat loss of the chamber, the cavity-style structure and the insulating asbestos are adopted.

2.1.2.5 Permeability Measurement and Humidity Control

In terms of the permeability as well as the effects of multiple cycles of drying and wetting on unsaturated soil mechanics, Goh et al. (2015) introduced a triaxial apparatus for direct measurement of permeability cooperated with shear strength tests on unsaturated soils under multiple cycles of drying and wetting. As shown in Fig. 7, the triaxial apparatus is mainly composed of a triaxial chamber, a loading system, pressure and flushing lines as well as measurement devices for load, pore pressure and volume change. During the drying and wetting processes as well as the shearing stage, valves A and F are used to control and measure the pore water pressure and the volume in the specimen. And during the unsaturated permeability test, valves A and F are used to control the different water pressures at the top and bottom of the specimen and measure the water flow through. Valve D is used to control the confining pressure during the whole testing process.

2.2 Triaxial Apparatus for Special Conditions

2.2.1 Triaxial Simulation on Rockburst

When the high-stress rocks are excavated, rockbursts may occur

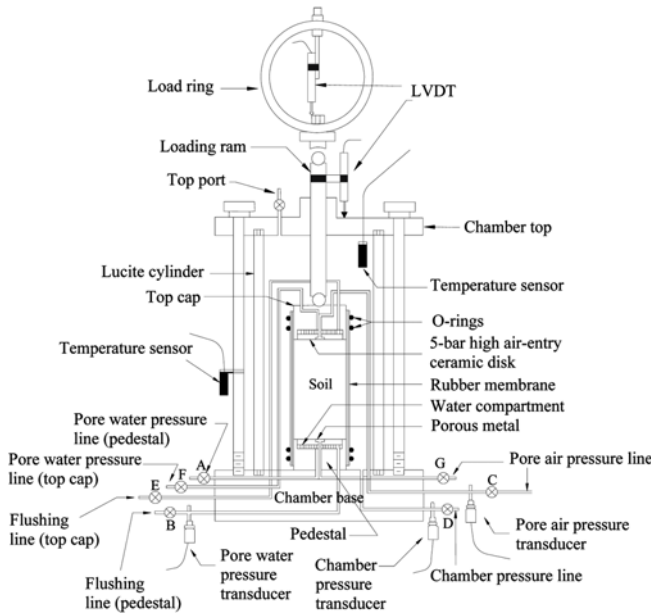


Fig. 7. Triaxial Apparatus for Permeability Measurement in Conjunction with Shear Strength Tests on Unsaturated Soils (after Goh et al., 2015)

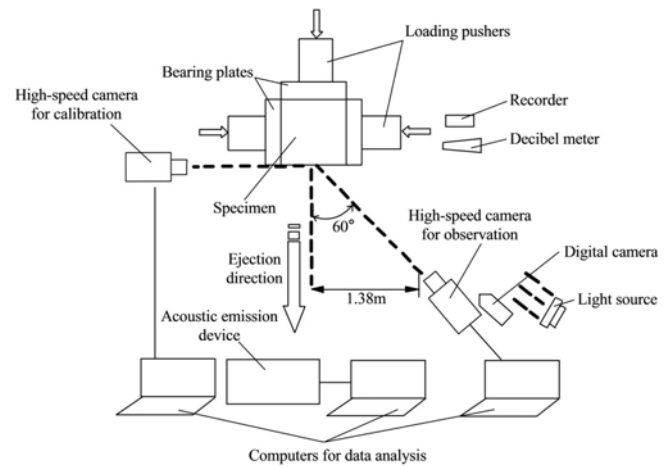


Fig. 8. The Layout of High-Speed Camera System (after Su et al., 2016)

due to the rapid release of strain energy. Rockburst can do great harm to the safety of underground engineering, including injuries, equipment damage and the delay of construction. Even worse, it can cause geological hazards such as instability and dynamic ejection of surrounding rocks. Therefore, rockburst has caused widespread concern in the field of geotechnical engineering (Meng et al., 2020; Gao et al., 2020; Sun et al., 2021).

Currently, most studies on rockburst focus on the energy of rocks and there are few studies on the impact of external disturbances (Wang and Park, 2001; Chen et al., 2019; Zhu et al., 2021). Actually, though the accumulation of strain energy in rocks is necessary for rockburst, it is external disturbance that plays a decisive role (He et al., 2014). Therefore, in order to have a deeper understanding of the impact of external disturbance on rockburst, it is necessary to simulate the stress state of surrounding rocks in laboratory, for which triaxial test is an effective method.

Actually, scholars have conducted a lot of research to effectively simulate the real stress state of surrounding rocks in practical engineering (Zhu et al., 2010; Yin et al., 2012; He et al., 2014; Yin et al., 2014b; Feng et al., 2018; Xu and Dai, 2018; Du et al., 2020; Wang et al., 2020; Li et al., 2020a; Zhang et al., 2021), but true triaxial tests that combine dynamic and static loads with one face free as well as the impact of external disturbances on rockburst are less studied. In response, Su et al. (2016) developed a true triaxial test system that can simultaneously simulate static loads and low-frequency cyclic loads, and the threshold value of the axial static stress, the third principal stress and the disturbance amplitude required for the occurrence of rockburst as well as the relationship between the kinetic energy of rockburst ejection and the frequency of external disturbances were studied. The main body of the system is a rigid press, which can carry out servo

loading independently in three orthogonal directions including six-sided compression, five-sided compression with one free face and six-sided compression with sudden unloading on one side. The system can not only perform static rockburst tests, but can also transmit loading commands of dynamic waves to the cylinders by servo control system to develop low-frequency dynamic loads. To record and measure the rockburst process, the system is also equipped with devices like high-speed cameras. The working process of high-speed camera system is shown in Fig. 8, through which the ejection velocity of rockburst can be obtained and the kinetic energy can be calculated accordingly to reflect the intensity and scale of the rockburst.

2.2.2 Temperature-Humidity Control Triaxial Test System

The temperature-humidity control triaxial test system is mainly used to study the mechanical properties of coarse-grained materials.

Coarse-grained materials are widely used in geotechnical structures such as subgrade engineering, rockfill dams and embankment due to a good compaction property and high shear strength (Liu et al., 2013; Zhou et al., 2020b). Since the mechanical properties of coarse-grained materials are not only related to the load, but also closely related to the environmental conditions such as the temperature and humidity (Zhang and Buscarnera, 2018; Zhou et al., 2020b), it is necessary to conduct triaxial tests under the conditions of accurate control of the temperature and humidity of coarse-grained materials in order to study their mechanical behavior under complex environmental conditions.

For the influence of environmental conditions on the mechanical properties of coarse-grained materials, scholars have conducted lots of research. Nie et al. (2021) studied the variation of resilient modulus of the coarse-grained soil under different moisture contents through a large-scale dynamic triaxial tests. Alonso et al. (2016) studied the yielding of coarse-grained materials through a relative humidity-controlled triaxial apparatus, in which the

relative humidity was maintained by a flow of moist air. Oldecop and Alonso (2001, 2003, 2007) controlled the relative humidity within the specimen by means of saturated saline solutions (namely vapour equilibrium technique) to make it possible to gradually change the specimen water content and suction during the test, and studied the straining process and the effect of water on the compressibility and collapse phenomena of rockfill, based on which models accounting for the features shown by rockfill in tests were proposed and extended. However, all these studies only achieve the humidity control and cannot study the coupling effect of temperature and humidity on coarse-grained materials. Zhang et al. (2014a, 2015) developed a weathering test apparatus that can test the deformation and shear strength behavior of coarse-grained materials under coupling actions of drying/wetting cycles, cooling/heating cycles and vertical loads, through which the deformation and shear strength of rockfill materials composed of soft siltstones under stress, cyclical drying/wetting and temperature variations were studied. However, the wetting of the specimen in the apparatus is achieved by saturating the specimen with the water from a tank, and the relative humidity cannot be controlled and varied. In addition, the maximum size of the specimen suitable for the apparatus is only 150 mm in diameter and 150 mm in height, which seems to be not enough for simulating the stress state of coarse-grained materials in practical engineering more authentically. To this end, Mao et al. (2021) developed a largescale triaxial apparatus for coarse-grained materials that can simultaneously control both temperature and humidity. The apparatus is mainly composed of three parts: loading and measuring system, temperature control system and humidity control system, as shown in Fig. 9.

Among them, the loading and measuring system is composed of reaction frame, pressure chamber, pressure actuator, pressure cylinder, displacement and pressure sensors and loading controller. The axial pressure is applied by the axial pressure actuator combined with the hydraulic pump, and the confining pressure is applied by the confining pressure actuator. The volume change of the specimen can be calculated by the change in the amount of water in pressure chamber. In order to control the relative humidity, a saturated aqueous salt solution is adopted in the system, which has been widely used for humidity control in

laboratory (Arai et al., 1976). As for temperature control, the system adopts the idea of controlling the water temperature in pressure chamber, so that the temperature of the specimen can be controlled through heat conduction. It is worth noting that the apparatus can load the specimen with the maximum size of 300 mm in diameter and 600 mm in height, and the maximum axial displacement can reach 250 mm.

2.2.3 Thermo-Mechanical Coupling Triaxial Test System

Triaxial study on thermal-mechanical coupling effect of rocks and soils is of great significance to geotechnical engineering projects like thermal energy storage and underground heat pipeline burying. The key to the thermo-mechanical coupling triaxial test is the control of the temperature, which commonly consists of three main methods as follows (Li et al., 2018; Xiong et al., 2018).

1. External temperature control (Wiebe et al., 1998; Sultan et al., 2002; Abuel-Naga et al., 2007), that is, the temperature of the sample is controlled by heating elements such as heating coils, heating plates or heater bands installed on the outer wall of the triaxial cell. Besides, temperature control achieved by placing the equipment in a high temperature environment (usually an incubator) is also regarded as an external temperature control method in this paper. The external temperature control has the longest time required for the sample to reach the target temperature. As for those achieved by placing the triaxial cell in an incubator, the costs for establishing a temperature-controlled laboratory are also higher. However, external temperature control does not need to change the internal structure of the triaxial cell, and the sample can be heated more evenly.
2. Internal temperature control (Demars, 1982; Kuntiwattanakul et al., 1995; Bruyn and Thimus, 1996; Sohm et al., 2012; Ng and Zhou, 2014; Ye et al., 2015; Cabalar and Clayton, 2016). The temperature of the sample is controlled by heating elements such as copper circulating coils or power heaters installed inside the triaxial cell. As for internal temperature control, the time required for the sample to reach the target temperature is short, but it is not easy to heat the fluid in triaxial cell evenly, thereby resulting in the uneven temperature distribution in the sample. Meanwhile, the structure of the triaxial cell should be modified so that the heating elements can be installed inside.
3. Combined temperature control (Xiong et al., 2018). The sample is heated both inside and outside the triaxial cell. For example, Xiong et al. (2018) adopted two curved heating plates close to the pressure chamber tube, and simultaneously heated the upper and lower ends of the sample and the fluid in pressure chamber by heating the upload pole and the piston rod. Combined temperature control is supposed to have the best effect in temperature control, but the required mechanism is usually more complicated and is not that easy to operate.

The advantages and disadvantages of the three temperature

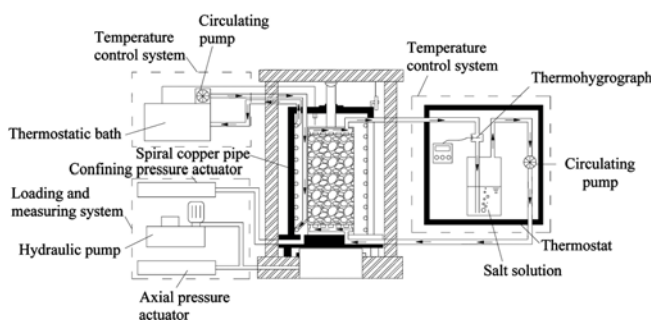


Fig. 9. Schematic Diagram of Temperature-Humidity Controlled Large Triaxial Apparatus for Coarse-grained Materials (after Mao et al., 2021)

Table 1. Comparison of the Three Temperature Control Methods

Methods	Control Effectiveness	Device Complexity	Experimental Operability
External	++	+	++
Internal	+	++	+++
Combined	+++	+++	+

Note: +++ high; ++ medium; + low

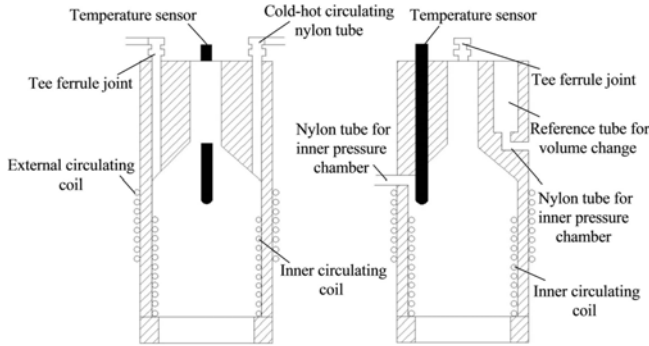


Fig. 10. Perpendicular Sections of Inner Pressure Chamber (after Li et al., 2018)

control methods are compared in Table 1.

Based on the advantages and disadvantages of the above-mentioned methods, Li et al. (2018) improved the temperature control system, as shown in Fig. 10. The inner pressure chamber made of acrylic has copper circulating coils wound both on the inner wall and the outside, and two tee ferrule joints are arranged on the top. The two ends of the copper circulating coil on the inner wall of the pressure chamber (inner circulating nylon coil) pass through the top of the pressure chamber and are respectively connected to the two tee ferrule joints. The connection of the copper circulating coil outside the pressure chamber (external circulating coil) is the same as that of the inner circulating coil. The remaining ports of the two tee ferrule joints are each connected to a cold-hot circulating nylon tube, and the two circulating nylon tubes are respectively connected to the inlet and outlet of the thermostatic bath. In addition, the improved inner pressure chamber is also equipped with a temperature sensor submerged in the degassed water in inner pressure chamber, which can monitor the temperature in real time.

In the improved temperature control system, the sample is completely surrounded by the inner circulating coil and can be heated evenly. Since the inner pressure chamber is installed in the outer pressure chamber filled with degassed water, the external circulating coil can simultaneously heat the degassed water outside the inner pressure chamber, which reduces not only the deformation of the inner pressure chamber caused by the temperature differences between inside and outside, but also the heat loss of the inner pressure chamber. Although the system is a combined temperature control system, it is simpler and easier to operate than conventional ones.

2.2.4 Stress-Seepage Coupling Triaxial Test System

Under natural conditions, rock masses usually coexist with groundwater. As an active and unfavorable factor, groundwater can not only produce seepage force, but also produce special mechanical effects through the coupling of water, rock and stress. This effect is achieved by changing the permeability of the rock mass, and thereby reducing its mechanical properties. Meanwhile, the change of the permeability will in return affect the stress distribution in rock mass, thus affecting its strength and deformation properties (Liu and Tang, 2008). Actually, the main cause for the failure of the Malpasset arch dam in France is just supposed to be the effect of stress-seepage coupling (Duffaut, 2013).

Using indoor triaxial tests to study the seepage laws of fractured rock masses under three-dimensional stress can more authentically reflect the actual states of natural rock masses. Chen et al. (2000) studied the hydraulic behavior of natural fractures and joints in granitic rock through triaxial tests, including the relationships among fracture offset as well as the mechanical aperture and hydraulic aperture under different stress conditions. Indraratna et al. (2001, 2003) studied the characterization of two-phase flow in a fractured rock mass through a two-phase (high-pressure) triaxial cell. Li et al. (2008) evaluated the influence of morphological properties of rock fractures on their hydro-mechanical behavior through shear-flow coupling tests. Koyama et al. (2008) conducted a series of coupled shear-flow tests for fracture replicas under normal stresses with visualization of fluid flow using a coupled shear-flow-tracer testing equipment, and the tests were simulated and compared by finite element method (FEM), through which the complex behavior of fluid flow in fracture samples were captured. Liu et al. (2019) performed a triaxial compression test of sandstone under high stress and high hydraulic pressure to analyze the special mechanical properties of deep rocks under high hydraulic pressure. Du et al. (2020) explored the behaviors in strength, deformation, permeability and failure mode of sandstone samples with two preexisting fissures through hydromechanical coupling triaxial tests. However, most of the existing studies focus on the seepage laws of fractured small-sized specimens under lower seepage forces, and the conclusions cannot completely reflect the real properties of largescale projects under high seepage forces. To solve the problem, Yin et al. (2014a) developed a true triaxial test system suitable for the study of large specimens under stress-seepage coupling effect with high seepage force, as shown in Fig. 11. The maximum size of the specimen that can be loaded is 400 mm × 200 mm × 200 mm. The system can achieve independent servo loading in three directions and the maximum water pressure is 5 MPa. Acoustic emission technique is also applied to monitor the evolution of the cracks in the specimen under the coupling effect of three-dimensional stress and water pressure in real time. The stress-seepage coupling true triaxial test system is composed of six subsystems, including axial loading subsystem, lateral loading subsystem, high-pressure water seepage subsystem, acoustic emission subsystem, data acquisition and control subsystem and triaxial box subsystem.

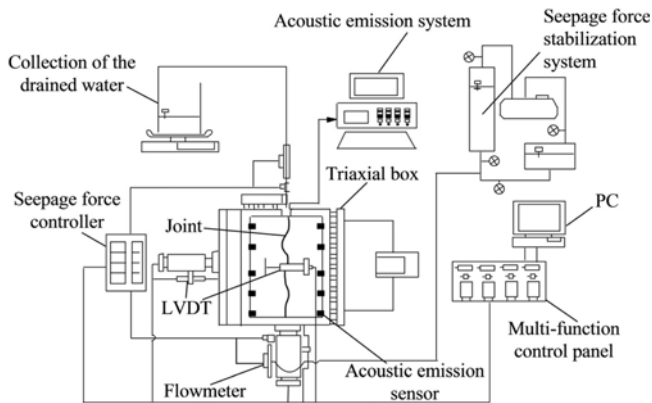


Fig. 11. Sketch Diagram of the True Triaxial Rock Test System for Coupled Stress-Seepage (after Yin et al., 2014a)

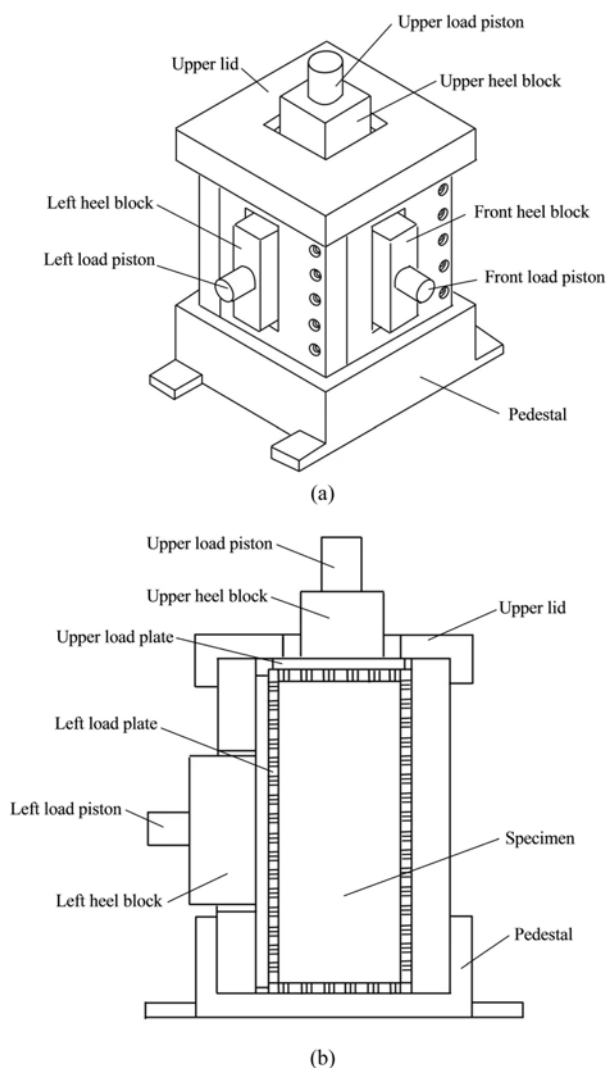


Fig. 12. Triaxial Box (after Yin et al., 2014a): (a) Perspective View, (b) Sectional View

The triaxial box, high-pressure water seepage system and acoustic emission monitoring are worth noting. As for the triaxial box, it is a true triaxial system that can realize independent loading

and deformation measurement in three orthogonal directions, as is shown in Fig. 12. During the test, the specimen is placed in the box and then servo loaded. The triaxial box is composed of a box body, heel blocks and gaskets, and the rigid-flexible structure is adopted in all directions. The top plate, rear plate and right plate of the box are made of high-rigidity steel and fixed on the frame through bolt connections, and can be easily disassembled and changed. The test box is sealed with new materials, which has a certain strength and can withstand a certain deformation as well, so that the high-pressure water can be well isolated. The greatest advantage of the triaxial box is that it can deform synchronously with the specimen in three orthogonal directions, which avoids the disturbances from different directions when the specimen is loaded. Besides, the triaxial box can be replaced to accommodate specimens of different sizes, especially those larger ones.

In terms of high water-pressure seepage, the innovation of the system is that it realizes effective sealing under high water pressure, which can guarantee a water pressure up to 5 MPa. Before the test, researchers put the specimen in a capsule and adequately sealed, and then water is injected from the bottom up. As for the acoustic emission system, its advantage lies in the realization of real-time, non-destructive monitoring of the fracture process. The principle and operation of acoustic emission will be introduced in detail in Section 3.1.

In recent years, many new techniques have been adopted in the field of stress-seepage coupling tests, most of which are the improvements of measurement or monitoring methods. For example, Rezaee et al. (2012) estimated the permeability of tight gas sands from mercury injection capillary pressure and nuclear magnetic resonance (NMR) data. Lv et al. (2020) studied the seepage characteristics of fractured coal and sandstone based on real-time micro-CT, and the rock samples under different stress states were scanned in real-time during the seepage testing. Zhao et al. (2022) investigated the pore and fracture development in coal under stress conditions based on NMR and fractal theory. In fact, just like the thermal-mechanical coupling test, the stress-seepage coupling test is essentially a multi-field coupling test. Therefore, these new techniques can also be applied to other multi-field coupling tests, which will serve as more effective methods for researchers to explore the mechanical behavior of rocks and soils under the action of multi-field coupling.

3. Triaxial Test Techniques

3.1 Acoustic Emission-Triaxial Joint Test Technique

Elastic waves emitted by microfracturing in materials are called acoustic emission (AE) (Ohtsu et al., 1991). The method that adopts AE to detect the fracture process of materials or components is AE technique. AE technique is a real-time monitoring method and a non-destructive testing technique (Li et al., 2015), and the acquired AE signals can be used to analyze the evolution of micro-cracks in brittle (or quasi-brittle) materials during loading process (Han et al., 2019).

The AE analysis includes parameter and waveform analysis

(Zhu et al., 2019), through which plenty of information on specimen fracture can be obtained. For example, the cracks of the specimen can be classified into tensile cracks and shear cracks according to the average frequency (AF) and the RA value (the ratio of the rise time to amplitude) (Ohtsu et al., 2007). Based on the b value (Colombo et al., 2003) or Ib value (Shiotani et al., 2001), the evolution of the cracks in the specimen can be analyzed. AE waveforms carry the information of both the sources and the medium (Burud and Kishen, 2020), and can provide insight into the sources and behavior of cracks that occur in materials (Farnam et al., 2015). Cluster analysis can be adopted to AE data to determine the failure stages of the specimen (Han et al., 2019). Besides, AE data can also be used to locate the micro-cracks (namely the AE sources) in the specimen (Xu et al., 2018; Li et al., 2019c; Xu et al., 2021).

Actually, AE technique has also been applied to triaxial tests. Lee and Rathnaweera (2016) found AE detection a powerful method for determining the phenomena of stable and unstable crack propagation of rocks under uniaxial and triaxial loading conditions. Yue et al. (2019) studied the mechanism of hydrofracturing process through a self-developed true triaxial hydraulic fracturing system combined with AE technique. Zhou et al. (2019) presented an innovative acousto-optic-sensing-based triaxial testing system for rocks, in which the acoustic emission sensors are used for measuring the internal damage of rock specimens during a load test. Pei et al. (2020) evaluated the rockburst proneness through AE characteristics of rocks under loading. Dong et al. (2022) studied the mechanical properties, failure modes, and damage evolution characteristics of the sandstone samples under uniaxial compression at different temperatures through AE technique. Lin et al. (2020) performed drained triaxial compression tests with the aid of AE technique, and the modified triaxial apparatus combined with AE devices is shown in Fig. 13. During tests, elastic waves emitted by micro-cracks in the specimen are detected by AE sensors attached on the surface of the specimen,

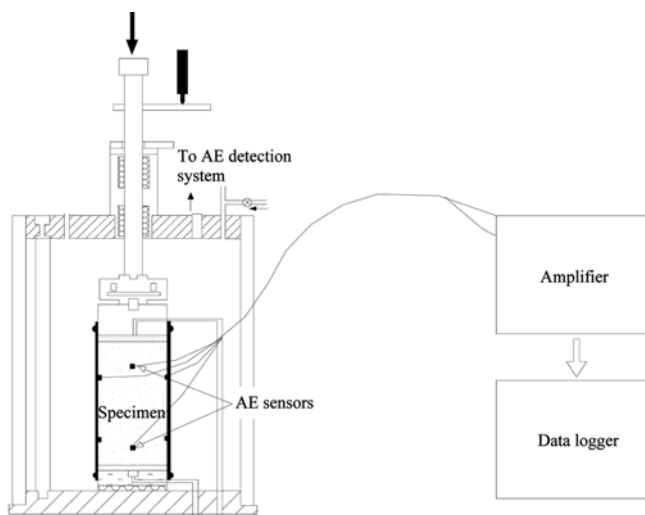


Fig. 13. Triaxial Apparatus Combined with AE Devices (after Lin et al., 2020)

and then the AE signals are amplified by the amplifier and collected by the data logger. Analyze the AE data stored in data logger, and the information on specimen fracture can be obtained.

3.2 Visualization Technology for Triaxial Tests

In traditional triaxial tests, due to the opacity of the medium, the fracture and deformation process as well as the migration of multi-phase matter in the specimen cannot be intuitively observed. To solve the problem, researchers have developed a variety of methods to realize visualization in recent years.

Otani et al. (2002) realized the visualization of the progressive failure of the sample in triaxial compression through the images obtained by an X-ray CT scanner. Seol et al. (2019) presented a testing assembly that combines pore-scale visualization and triaxial test capability of methane hydrate-bearing sediments. Li et al. (2020c) realized three-dimensional (3D) visualization of coal fracture dynamic evolution under uniaxial and triaxial compression based on X-ray micro-Computed Tomography (X-ray μ CT). Li et al. (2021a) introduced a new technique for the visualization of a deforming specimen during triaxial tests based on a full-field deformation measurement system with the aid of a self-developed software package GeoTri3D. Jiang et al. (2021) realized 3D visualization of coal and shale through computed tomography (CT) scanning and real-time AE signal monitoring, and studied the evolution of pores and fractures in reservoir rocks under triaxial stress conditions. Of course, the NMR is also a visualization technology that can be applied to triaxial tests. In addition, the field of geotechnical tests has been trying to use transparent geotechnical materials to visualize the testing process in recent decades.

Transparent geotechnical material is a kind of artificial transparent material that is similar to natural soils in terms of strength and deformation properties. There are mainly three families of transparent materials developed for modeling sand and clays, which are made of amorphous silica powder, transparent silica gels and Aquabeads to represent natural clays, sand as well as very weak sediments and the flow in soils respectively (Iskander, 2010). In addition, pore fluids like mineral oil and the mixture of calcium bromide and water are also adopted to establish transparent models (Iskander, 2010). Since the simulated soils are transparent, researchers can easily obtain the deformation and failure information in the sample by optical means. In recent decades, transparent soils have been widely used in studying the infiltration (Siemens et al., 2013) and the dynamic properties (Kong et al., 2016) of soils, as well as the interaction between tunnel excavation (Sun and Liu, 2014; Li et al., 2020b), anchor keying (Song et al., 2009), geogrid (Ezzein and Bathurst, 2014; Derksen et al., 2021; Chen et al., 2021a), piles (Ni et al., 2010; Hird et al., 2011; Stanier et al., 2012; Liu et al., 2020) and soils. Compared with other visualization methods such as NMR and CT, transparent materials can achieve favorable effects at a lower cost, thus attracting much attention in geotechnical tests. Actually, new techniques like 3D-printing (Li et al., 2021b) have also been introduced to make transparent soils in recent years so that researchers can consider the effects of factors like the shapes of soil particles on

the macromechanical soil properties.

4. Prospects

From the above-mentioned new triaxial test instruments and test techniques, it can be found that the current triaxial tests have the following developing trends.

4.1 Diversification in Functions

The functions of triaxial test instruments tend to be diversified. The current triaxial test instruments are no longer limited to obtaining the strength index of the rocks and soils through loading, but have begun to pay attention to the mechanical properties of special soils (rocks) and soils (rocks) under special conditions like geologic hazards and multi-field coupling.

As for special soils, in addition to the triaxial study on hydrate sediments (Priest et al., 2015; Zhou et al., 2020a) and unsaturated soils (Cui and Delage, 1996; Wulfsohn et al., 1998; Ng et al., 2002; Cai et al., 2014; Goh et al., 2015; Zheng et al., 2020), special soils like frozen soils are also studied through triaxial tests (Yao et al., 2013). In terms of special conditions of geologic hazards, besides rockburst (Su et al., 2016), other phenomena like water inrush have been investigated. Li et al. (2019d) studied the mechanism of water inrush through a large-scale true triaxial geomechanical model test. Yang et al. (2019) developed a true triaxial geomechanical model test apparatus, which can be used to study the precursory information of water inrush from impermeable rock mass failure as well as the solid-fluid interaction of the surrounding rock mass and water. As for special conditions of multi-field coupling, there are triaxial apparatus for thermo-humidity coupling (Mao et al., 2021), thermo-mechanical coupling (Li et al., 2018; Li et al., 2021c) and stress-seepage coupling (Yin et al., 2014a; Frash et al., 2016). Feng et al. (2021) also introduced a true triaxial test system for microwave-induced fracturing of hard rocks, through which the coupling of true triaxial stress and microwave can be achieved. Besides, conditions in some special engineering activities, such as deep geological CO₂ sequestration, have also been considered. For example, Ranjith and Perera (2011) presented a new high-pressure triaxial apparatus that can provide the high confining and fluid injection pressures and elevated temperatures expected for deep geological CO₂ sequestration, which can be used to conduct mechanical and permeability testing on intact or fractured natural rock samples or synthetic rock samples subjected to high-pressure injection of up to three fluid phases (gas and/or liquid) at high pressures and temperatures corresponding to field conditions.

4.2 Improvements in Specimen Performance

The testing performance of the specimen is improved.

First, larger specimens are adopted in triaxial loading, so that the test results are closer to real conditions. For example, the temperature-humidity controlled large triaxial apparatus developed by Mao et al. (2021) can load the specimen with the maximum size of 300 mm in diameter and 600 mm in height. The maximum

size of the specimen that can be loaded by the true triaxial rock test system for coupled stress-seepage developed by Yin et al. (2014a) is 400 mm × 200 mm × 200 mm. Chen et al. (2021b) developed a large-scale true triaxial seepage apparatus that can load the specimen with a maximal size of 1,050 mm × 550 mm × 550 mm. Yang et al. (2019) developed a true triaxial geomechanical model test apparatus, and the size of the specimen can reach 1,500 mm × 1,000 mm × 1,000 mm.

Besides, specimens are also improved to be more convenient for observation and monitoring. Typically, the adoption of transparent geotechnical materials (Song et al., 2009; Ni et al., 2010; Hird et al., 2011; Stanier et al., 2012; Siemens et al., 2013; Ezzein and Bathurst, 2014; Sun and Liu, 2014; Kong et al., 2016; Liu et al., 2020; Li et al., 2020b; Derksen et al., 2021; Chen et al., 2021a) instead of conventional samples allows researchers to more intuitively grasp the mechanical behavior of rocks and soils.

4.3 Visualization and Real-Time Monitoring

Monitoring methods tend to be visible and real-time, and can obtain more internal and microscopic information of the specimen.

As described in Section 3, visualization can be achieved by techniques like CT (Otani et al., 2002; Li et al., 2020c; Jiang et al., 2021). Besides, due to the localization function, AE technique can also be considered a method for visualization. In terms of real-time monitoring, besides the AE technique, which can realize real-time monitoring of the micro-cracks both inside and on the surface of a specimen, other techniques including digital image correlation (DIC) and X-ray CT are also adopted. Rechenmacher (2006) obtained nearly continuous (both spatially and temporally) record of displacement evolution through the non-destructive displacement measurement technique of DIC. Watanabe et al. (2012) developed a method of tracking soil particles through CT images so that the displacements in sand in three dimensions under triaxial compression can be obtained. Wang et al. (2021b) applied the X-ray CT detections to the uniaxial and triaxial compression of coal samples and the dynamic evolution of the fractures during the deformation can be revealed. Actually, several different real-time monitoring techniques can be combined to form a real-time monitoring system, so that more information can be collected. For example, Feng et al. (2021) developed a dynamic monitoring system for true triaxial tests, which includes the infrared thermometry technique for monitoring rock surface temperature, the distributed optic fiber sensing technique for monitoring temperature in borehole in rock, and the AE technique and two-dimensional digital speckle correlation technique for monitoring the evolution of thermal damage and the rock fracturing process.

4.4 Error Elimination and High Accuracy

The origin and influence of the errors are studied, so that they can be eliminated to guarantee the precision of triaxial tests.

There are mainly two error sources in triaxial tests, one is the manual operation, called manmade factors, and the other is the

apparatus itself, called systemic factors. Errors caused by manmade factors can be eliminated by improving the automation of test operations and minimizing manual operations. Actually, researchers have been trying to improve the automation in aspects like measurement and data logging. For example, Lewin (1971) transformed the volume change into the linear movement of a piston, which can then either be measured on a dial gauge or be used to operate an electronic displacement transducer for direct data logging.

In addition to those caused by manmade factors, errors caused by systemic factors also have an impact on test results. At present, the influence of some systemic factors has been clarified in research. Many scholars have studied the effects of rubber membrane in triaxial tests such as the effects on measured deviatoric stress and volume change, and Raghunandan et al. (2015) have made a comprehensive review on it. Leroueil et al. (1988) evaluated the influence of the drainage capacity of filter papers on the consolidation and shear processes in triaxial tests. Lefebvre and LeBoeuf (1987) studied the influence of the strain rate and load cycles on the undrained shear strength of different clays in monotonic and cyclic triaxial tests. Li and Zhang (2019) systematically evaluated the factors concerning the accuracy of the photogrammetry-based deformation measurement method, including mesh density and pattern, interpolation technique and system parameters like the refractive index of the confining medium as well as the refractive index and thickness of the triaxial chamber wall. Based on the studies, some methods that can eliminate the systemic errors have been proposed. Zhu and Anderson (1998) briefly described the methods for the correction of the errors caused by membrane compliance, membrane resistance and variations in cross-sectional area and developed an overall correction procedure based on the soil behavior observed during triaxial tests. Dihoru et al. (2005) proposed a neural network (NN) approach to predict the errors in true triaxial apparatus with flexible boundaries (TTAF) that may affect the displacements of the sample, which can effectively overcome the difficulty associated with a complex set of factors of influence like the effects of the sample membrane and the pressurizing cushion, the non-uniform spatial stiffness of the frame of the apparatus, and the electronic errors. Fang (2013) proposed a method to exclude data with gross errors so that the only strength line as well as cohesion and friction angle can be determined accurately. Therefore, it is possible to improve the triaxial tests and data processing accordingly to eliminate the systemic errors. Of course, strategies for both manmade errors and systemic errors can be adopted together, so that both the manmade and systemic errors can be eliminated.

5. Conclusions

The paper introduced several new types of triaxial test instruments suitable for the study on the mechanical properties of special soils and soils (rocks) under special conditions. The application of AE and visualization techniques in triaxial tests has also been introduced. Furthermore, the developing trends were discussed.

The conclusions are summarized as follows:

1. Compared with conventional triaxial apparatuses, newly developed apparatuses in recent decades can be classified into two categories: the apparatuses for testing special soils (rocks) and those for soils (rocks) under special conditions. Representative special soils (rocks) include hydrate sediments and unsaturated soils. While special conditions can be classified into geologic hazards like rockburst and multi-field coupling like thermo-humidity coupling, thermo-mechanical coupling and stress-seepage coupling.
2. Techniques adopted in triaxial tests usually aim at achieving real-time monitoring and the visualization of the specimen behavior. AE technique is a real-time and non-destructive monitoring technique that can be used to analyze the evolution of micro-cracks in the specimen during triaxial tests. Commonly used methods for visualization include CT, geotechnical testing models established with transparent materials, etc., and transparent materials can achieve favorable effects at a lower cost.
3. The functions of triaxial test instruments tend to be diversified, and the testing performance of the specimen is improved. The monitoring methods adopted in triaxial tests tend to be visible and real-time, and can obtain more internal and microscopic information of the specimen. In addition, the triaxial tests tend to be more accurate as the origin and influence of the errors are deeply studied and effectively eliminated.

The review is expected to provide references for further study of triaxial tests in both instruments and techniques.

Acknowledgments

The authors acknowledge the support of the National Natural Science Foundation of China (No.52178342) and Natural Science Foundation of Tianjin City (No.19JCYBJC22200).

ORCID

Not Applicable

References

- Abuel-Naga HM, Bergado DT, Lim BF (2007) Effect of temperature on shear strength and yielding behavior of soft Bangkok clay. *Soils and Foundations* 47(3):423-436, DOI: [10.3208/sandf.47.423](https://doi.org/10.3208/sandf.47.423)
- Alonso EE, Romero EE, Ortega E (2016) Yielding of rockfill in relative humidity-controlled triaxial experiments. *Acta Geotechnica* 11:455-477, DOI: [10.1007/s11440-016-0437-9](https://doi.org/10.1007/s11440-016-0437-9)
- Arai C, Hosaka S, Murase K, Sano Y (1976) Measurements of the relative humidity of saturated aqueous salt solutions. *Journal of Chemical Engineering of Japan* 9(4):328-330, DOI: [10.1252/jcej.9.328](https://doi.org/10.1252/jcej.9.328)
- Bell JM (1965) Stress-strain characteristics of cohesionless granular materials subjected to statically applied homogeneous loads in an open system. PhD Thesis, California Institute of Technology, California, USA

- Bruyn DD, Thimus JF (1996) The influence of temperature on mechanical characteristics of Boom clay: The results of an initial laboratory programme. *Engineering Geology* 41:117-126, DOI: [10.1016/0013-7952\(95\)00029-1](https://doi.org/10.1016/0013-7952(95)00029-1)
- Burud N, Kishen JC (2020) Damage detection using wavelet entropy of acoustic emission waveforms in concrete under flexure. *Structural Health Monitoring*, DOI: [10.1177/1475921720957096](https://doi.org/10.1177/1475921720957096)
- Cabalar AF, Clayton C (2016) Effect of temperature on triaxial behavior of a sand with disaccharide. *Periodica Polytechnica Civil Engineering* 60(4):603-609, DOI: [10.3311/PPci.8631](https://doi.org/10.3311/PPci.8631)
- Cai GQ, Zhao CG, Li J, Liu Y (2014) A new triaxial apparatus for testing soil water retention curves of unsaturated soils under different temperatures. *Journal of Zhejiang University-SCIENCE A (Applied Physics & Engineering)* 15(5):364-373, DOI: [10.1631/jzus.A1300358](https://doi.org/10.1631/jzus.A1300358)
- Chen CH, Chen SS, Mei SA, Tang Y, Li YH (2021b) A large-scale true triaxial seepage apparatus for evaluating impact under high stress state and high hydraulic heads. *Geotechnical Testing Journal* 44(6):1617-1634, DOI: [10.1520/GTJ20200070](https://doi.org/10.1520/GTJ20200070)
- Chen JF, Gu ZA, Rajesh S, Yu SB (2021a) Pullout behavior of triaxial geogrid embedded in a transparent soil. *International Journal of Geomechanics* 21(3):04021003, DOI: [10.1061/\(ASCE\)GM.1943-5622.0001936](https://doi.org/10.1061/(ASCE)GM.1943-5622.0001936)
- Chen Z, Narayan SP, Yang Z, Rahman SS (2000) An experimental investigation of hydraulic behaviour of fractures and joints in granitic rock. *International Journal of Rock Mechanics & Mining Sciences* 37:1061-1071, DOI: [10.1016/S1365-1609\(00\)00039-3](https://doi.org/10.1016/S1365-1609(00)00039-3)
- Chen ZY, Su GS, Ju JW, Jiang JQ (2019) Experimental study on energy dissipation of fragments during rockburst. *Bulletin of Engineering Geology and the Environment* 78(7):5369-5386, DOI: [10.1007/s10064-019-01463-9](https://doi.org/10.1007/s10064-019-01463-9)
- Choi C, Arduino P, Harney MD (2008) Development of a true triaxial apparatus for sands and gravels. *Geotechnical Testing Journal* 31(1): 32-44, DOI: [10.1520/GTJ100217](https://doi.org/10.1520/GTJ100217)
- Choi JH, Dai S, Lin JS, Seol YK (2018) Multistage triaxial tests on laboratory-formed methane hydrate-bearing sediments. *Journal of Geophysical Research: Solid Earth* 123:3347-3357, DOI: [10.1029/2018JB015525](https://doi.org/10.1029/2018JB015525)
- Colombo IS, Main IG, Forde MC (2003) Assessing damage of reinforced concrete beam using “b-value” analysis of acoustic emission signals. *Journal of Materials in Civil Engineering* 15(3):280-286, DOI: [10.1061/\(ASCE\)0899-1561\(2003\)15:3\(280\)](https://doi.org/10.1061/(ASCE)0899-1561(2003)15:3(280))
- Cui YJ, Delage P (1996) Yielding and plastic behaviour of an unsaturated compacted silt. *Géotechnique* 46(2):291-311, DOI: [10.1680/geot.1996.46.2.291](https://doi.org/10.1680/geot.1996.46.2.291)
- Davies JT, Rideal EK (1963) *Interfacial phenomena* (second edition). Academic Press, Inc., New York, NY, USA, DOI: [10.1016/B978-0-12-206056-4.X5001-2](https://doi.org/10.1016/B978-0-12-206056-4.X5001-2)
- Demars KR (1982) Soil volume changes induced by temperature cycling. *Canadian Geotechnical Journal* 19:188-194, DOI: [10.1139/t82-021](https://doi.org/10.1139/t82-021)
- Derksen J, Ziegler M, Fuentes R (2021) Geogrid-soil interaction: A new conceptual model and testing apparatus. *Geotextiles and Geomembranes* 49(5):1393-1406, DOI: [10.1016/j.geotexmem.2021.05.011](https://doi.org/10.1016/j.geotexmem.2021.05.011)
- Desrues J, Chambon R, Mokni M, Mazerolle F (1996) Void ratio evolution inside shear bands in triaxial sand specimens studied by computed tomography. *Géotechnique* 46(3):529-546, DOI: [10.1680/geot.1996.46.3.529](https://doi.org/10.1680/geot.1996.46.3.529)
- Dihoru L, Wood DM, Sadek T, Lings M (2005) A neural network for error prediction in a true triaxial apparatus with flexible boundaries. *Computers and Geotechnics* 32:59-71, DOI: [10.1016/j.compgeo.2005.01.003](https://doi.org/10.1016/j.compgeo.2005.01.003)
- Dong L, Li YL, Liao HL, Liu CL, Chen Q, Hu GW, Liu LL, Meng QG (2020) Strength estimation for hydrate-bearing sediments based on triaxial shearing tests. *Journal of Petroleum Science and Engineering* 184:106478, DOI: [10.1016/j.petrol.2019.106478](https://doi.org/10.1016/j.petrol.2019.106478)
- Dong XH, Yang GS, Liu S (2022) Experimental study on AE response and damage evolution characteristics of frozen sandstone under uniaxial compression. *Cold Regions Science and Technology* 193: 103424, DOI: [10.1016/j.coldregions.2021.103424](https://doi.org/10.1016/j.coldregions.2021.103424)
- Du H, Song DQ, Chen Z, Guo ZZ (2020) Experimental study of the influence of structural planes on the mechanical properties of sandstone specimens under cyclic dynamic disturbance. *Energy Science & Engineering* 1-21, DOI: [10.1002/ese3.794](https://doi.org/10.1002/ese3.794)
- Du YT, Li TC, Li WT, Ren YD, Wang G, He P (2020) Experimental study of mechanical and permeability behaviors during the failure of sandstone containing two preexisting fissures under triaxial compression. *Rock Mechanics and Rock Engineering* 53:3673-3697, DOI: [10.1007/s00603-020-02119-x](https://doi.org/10.1007/s00603-020-02119-x)
- Duffaut P (2013) The traps behind the failure of Malpasset arch dam, France, in 1959. *Journal of Rock Mechanics and Geotechnical Engineering* 5:335-341, DOI: [10.1016/j.jrmge.2013.07.004](https://doi.org/10.1016/j.jrmge.2013.07.004)
- Ezzein FM, Bathurst RJ (2014) A new approach to evaluate soil-geosynthetic interaction using a novel pullout test apparatus and transparent granular soil. *Geotextiles and Geomembranes* 42:246-255, DOI: [10.1016/j.geotexmem.2014.04.003](https://doi.org/10.1016/j.geotexmem.2014.04.003)
- Fang W (2013) Gross error elimination and index determination of shearing strength parameters in triaxial test. *Applied Mechanics and Materials* 353-356:152-158, DOI: [10.4028/www.scientific.net/AMM.353-356.152](https://doi.org/10.4028/www.scientific.net/AMM.353-356.152)
- Farnam Y, Geiker MR, Bentz D, Weiss J (2015) Acoustic emission waveform characterization of crack origin and mode in fractured and ASR damaged concrete. *Cement & Concrete Composites* 60:135-145, DOI: [10.1016/j.cemconcomp.2015.04.008](https://doi.org/10.1016/j.cemconcomp.2015.04.008)
- Feng P, Dai F, Liu Y, Xu NW, Fan PX (2018) Effects of coupled static and dynamic strain rates on mechanical behaviors of rock-like specimens containing pre-existing fissures under uniaxial compression. *Canadian Geotechnical Journal* 55:640-652, DOI: [10.1139/cgj-2017-0286](https://doi.org/10.1139/cgj-2017-0286)
- Feng XT, Zhang JY, Yang CX, Tian J, Lin F, Li SP, Su XX (2021) A novel true triaxial test system for microwave-induced fracturing of hard rocks. *Journal of Rock Mechanics and Geotechnical Engineering* 13:961-971, DOI: [10.1016/j.jrmge.2021.03.008](https://doi.org/10.1016/j.jrmge.2021.03.008)
- Frash LP, Carey JW, Zhou L, Rougier E, Ickes T, Viswanathan HS (2016) High-stress triaxial direct-shear fracturing of Utica shale and in situ X-ray microtomography with permeability measurement. *Journal of Geophysical Research: Solid Earth* 121(7):5493-5508, DOI: [10.1002/2016JB012850](https://doi.org/10.1002/2016JB012850)
- Fredlund DG, Rahardjo H (1993) *Soil Mechanics for unsaturated soils*. John Wiley & Sons, Inc., New York, NY, USA, DOI: [10.1002/9780470172759](https://doi.org/10.1002/9780470172759)
- Gao L, Gao F, Xing Y, Zhang ZZ (2020) An energy preservation index for evaluating the rockburst potential based on energy evolution. *Energies* 13:3636, DOI: [10.3390/en13143636](https://doi.org/10.3390/en13143636)
- Garga VK, Zhang H (1997) Volume changes in undrained triaxial tests on sands. *Canadian Geotechnical Journal* 34:762-772, DOI: [10.1139/t97-038](https://doi.org/10.1139/t97-038)
- Goh SG, Rahardjo H, Leong EC (2015) Modification of triaxial apparatus for permeability measurement of unsaturated soils. *Soils and Foundations* 55(1):63-73, DOI: [10.1016/j.sandf.2014.12.005](https://doi.org/10.1016/j.sandf.2014.12.005)
- Green GE (1969) Strength and compressibility of granular materials under generalized strain conditions. PhD Thesis, University of London,

- London, UK
- Hambly EC (1969) A new true triaxial apparatus. *Geotechnique* 19(2): 307-309, DOI: [10.1680/geot.1969.19.2.307](https://doi.org/10.1680/geot.1969.19.2.307)
- Han QH, Yang G, Xu J, Fu ZW, Lacidogna G, Carpinteri A (2019) Acoustic emission data analyses based on crumb rubber concrete beam bending tests. *Engineering Fracture Mechanics* 210:189-202, DOI: [10.1016/j.engfracmech.2018.05.016](https://doi.org/10.1016/j.engfracmech.2018.05.016)
- He MC, Liu DQ, Gong WL, Wang CC, Kong J, Du S, Zhang K (2014) Development of a testing system for impact rockbursts. *Chinese Journal of Rock Mechanics and Engineering* 33(9):1729-1739, DOI: [10.13722/j.cnki.jrme.2014.09.001](https://doi.org/10.13722/j.cnki.jrme.2014.09.001) (in Chinese)
- Hird CC, Ni Q, Guymier I (2011) Physical modelling of deformations around piling augers in clay. *Geotechnique* 61(11):993-999, DOI: [10.1680/geot.9.T.028](https://doi.org/10.1680/geot.9.T.028)
- Hoyos LR, Macari EJ (2001) Development of a stress/suction-controlled true triaxial testing device for unsaturated soils. *Geotechnical Testing Journal* 24(1):5-13, DOI: [10.1520/GTJ11277J](https://doi.org/10.1520/GTJ11277J)
- Hoyos LR, Pérez-Ruiz DD, Puppala AJ (2012) Refined true triaxial apparatus for testing unsaturated soils under suction-controlled stress paths. *International Journal of Geomechanics* 12(3):281-291, DOI: [10.1061/\(ASCE\)GM.1943-5622.0000138](https://doi.org/10.1061/(ASCE)GM.1943-5622.0000138)
- Hyodo M, Li YH, Yoneda J, Nakata Y, Yoshimoto N, Nishimura A, Song YC (2013) Mechanical behavior of gas-saturated methane hydrate-bearing sediments. *Journal of Geophysical Research: Solid Earth* 118:5185-5194, DOI: [10.1002/2013JB010233](https://doi.org/10.1002/2013JB010233)
- Ibsen LB, Praastrup U (2002) The danish rigid boundary true triaxial apparatus for soil testing. *Geotechnical Testing Journal* 25(3):254-265, DOI: [10.1520/GTJ11096J](https://doi.org/10.1520/GTJ11096J)
- Indraratna B, Ranjith PG (2001) Laboratory measurement of two-phase flow parameters in rock joints based on high pressure triaxial testing. *Journal of Geotechnical and Geoenvironmental Engineering* 127(6): 530-542, DOI: [10.1061/\(ASCE\)1090-0241\(2001\)127:6\(530\)](https://doi.org/10.1061/(ASCE)1090-0241(2001)127:6(530))
- Indraratna B, Ranjith PG, Price JR, Gale W (2003) Two-phase (Air and Water) flow through rock joints: Analytical and experimental study. *Journal of Geotechnical and Geoenvironmental Engineering* 129(10): 918-928, DOI: [10.1061/\(ASCE\)1090-0241\(2003\)129:10\(918\)](https://doi.org/10.1061/(ASCE)1090-0241(2003)129:10(918))
- Ishikawa T, Zhang Y, Tokoro T, Miura S (2014) Medium-size triaxial apparatus for unsaturated granular subbase course materials. *Soils and Foundations* 54 (1):67-80, DOI: [10.1016/j.sandf.2013.12.007](https://doi.org/10.1016/j.sandf.2013.12.007)
- Iskander M (2010) Modelling with transparent soils. Springer-Verlag, Berlin Heidelberg, Germany, DOI: [10.1007/978-3-642-02501-3](https://doi.org/10.1007/978-3-642-02501-3)
- Ismail MA, Sharma SS, Fahey MT (2005) A small true triaxial apparatus with wave velocity measurement. *Geotechnical Testing Journal* 28(2):113-122, DOI: [10.1520/GTJ12648](https://doi.org/10.1520/GTJ12648)
- Jiang CB, Liu XD, Wang WS, Wei WH, Duan MK (2021) Three-dimensional visualization of the evolution of pores and fractures in reservoir rocks under triaxial stress. *Powder Technology* 378:585-592, DOI: [10.1016/j.powtec.2020.10.013](https://doi.org/10.1016/j.powtec.2020.10.013)
- Kjellman W (1936) Report on an apparatus for consummate investigation of the mechanical properties of soils. Proceedings of the 1st international conference on soil mechanics and foundation engineering, June 22, Cambridge, UK, 16-20 16-20
- Kong GQ, Zhou LD, Wang ZT, Yang G, Li H (2016) Shear modulus and damping ratios of transparent soil manufactured by fused quartz. *Materials Letters* 182:257-259, DOI: [10.1016/j.matlet.2016.07.012](https://doi.org/10.1016/j.matlet.2016.07.012)
- Koyama T, Li B, Jiang YJ, Jing LR (2008) Coupled shear-flow tests for rock fractures with visualization of the fluid flow and their numerical simulations. *International Journal of Geotechnical Engineering* 2:215-227, DOI: [10.3328/IJGE.2008.02.03.215-227](https://doi.org/10.3328/IJGE.2008.02.03.215-227)
- Kuntiwattanakul P, Towhata I, Ohishi K, Seko I (1995) Temperature effects on undrained shear characteristics of clay. *Soils and Foundations* 35:147-162, DOI: [10.3208/sandf1972.35.147](https://doi.org/10.3208/sandf1972.35.147)
- Lee B, Rathnaweera TD (2016) Stress threshold identification of progressive fracturing in Bukit Timah granite under uniaxial and triaxial stress conditions. *Geomechanics and Geophysics for Geo-Energy and Geo-Resources* 2:301-330, DOI: [10.1007/s40948-016-0037-z](https://doi.org/10.1007/s40948-016-0037-z)
- Lefebvre G, LeBoeuf D (1987) Rate effects and cyclic loading of sensitive clays. *Journal of Geotechnical Engineering* 113(5):476-489, DOI: [10.1061/\(ASCE\)0733-9410\(1987\)113:5\(476\)](https://doi.org/10.1061/(ASCE)0733-9410(1987)113:5(476))
- Leroueil S, Tavenas F, La Rochelle P, Tremblay M (1988) Influence of filter paper and leakage on triaxial testing. Proceedings of symposium on advanced triaxial testing of soil and rock, January 1, Louisville, KY, USA, DOI: [10.1520/STP29078S](https://doi.org/10.1520/STP29078S)
- Lewin PI (1971) Use of servo mechanisms for volume change measurement and k_0 consolidation. *Geotechnique* 21(3):259-262, DOI: [10.1680/geot.1971.21.3.259](https://doi.org/10.1680/geot.1971.21.3.259)
- Li B, Jiang YJ, Koyama T, Jing LR, Tanabashi Y (2008) Experimental study of the hydro-mechanical behavior of rock joints using a parallel-plate model containing contact areas and artificial fractures. *International Journal of Rock Mechanics & Mining Sciences* 45:362-375, DOI: [10.1016/j.ijrmms.2007.06.004](https://doi.org/10.1016/j.ijrmms.2007.06.004)
- Li CH, Kong GQ, Zhang XR, Liu HL, Wang LH (2021c) Thermomechanical properties of sand-structure interface using temperature-controlled triaxial instrument. *Canadian Geotechnical Journal* 58:248-260, DOI: [10.1139/cgj-2020-0026](https://doi.org/10.1139/cgj-2020-0026)
- Li DL, Wang Z, Liang DQ, Wu XP (2019a) Effect of clay content on the mechanical properties of hydrate-bearing sediments during hydrate production via depressurization. *Energies* 12:2684, DOI: [10.3390/en12142684](https://doi.org/10.3390/en12142684)
- Li DS, Chen Z, Feng QM, Wang YL (2015) Damage analysis of CFRP-confined circular concrete-filled steel tubular columns by acoustic emission techniques. *Smart Materials and Structures* 24:085017, DOI: [10.1088/0964-1726/24/8/085017](https://doi.org/10.1088/0964-1726/24/8/085017)
- Li DY, Xiao P, Han ZY, Zhu QQ (2020a) Mechanical and failure properties of rocks with a cavity under coupled static and dynamic loads. *Engineering Fracture Mechanics* 225:106195, DOI: [10.1016/j.engfracmech.2018.10.021](https://doi.org/10.1016/j.engfracmech.2018.10.021)
- Li J, Wang Y, Kong LW, Wang MY, Cheng P, Ma YZ (2018) Development and preliminary application of a new temperature-controlled triaxial test system for unsaturated soils. *Chinese Journal of Geotechnical Engineering* 40(3):468-474, DOI: [10.11779/CJGE201803010](https://doi.org/10.11779/CJGE201803010) (in Chinese)
- Li JJ, Huang J, Niu JG, Wan CJ (2019c) Mesoscopic study on axial compressive damage of steel fiber reinforced lightweight aggregate concrete. *Construction and Building Materials* 196:14-25, DOI: [10.1016/j.conbuildmat.2018.11.135](https://doi.org/10.1016/j.conbuildmat.2018.11.135)
- Li K, Liu RM, Kong L, Zhao XB (2019b) Modeling the mechanical behavior of gas hydrate bearing sediments based on unified hardening framework. *Geotechnical and Geological Engineering* 37:2893-2902, DOI: [10.1007/s10706-019-00804-5](https://doi.org/10.1007/s10706-019-00804-5)
- Li L, Li P, Cai Y, Lu Y (2021a) Visualization of non-uniform soil deformation during triaxial testing. *Acta Geotechnica* 16:3439-3454, DOI: [10.1007/s11440-021-01310-w](https://doi.org/10.1007/s11440-021-01310-w)
- Li L, Zhang X (2019) Factors influencing the accuracy of the photogrammetry-based deformation measurement method. *Acta Geotechnica* 14: 559-574, DOI: [10.1007/s11440-018-0663-4](https://doi.org/10.1007/s11440-018-0663-4)
- Li L, Zhang X, Chen G, Lytton R (2016) Measuring unsaturated soil deformations during triaxial testing using a photogrammetry-based method. *Canadian Geotechnical Journal* 53:472-489, DOI: [10.1139/cgj-2015-0038](https://doi.org/10.1139/cgj-2015-0038)

- Li SC, Gao CL, Zhou ZQ, Li LP, Wang MX, Yuan YC, Wang J (2019d) Analysis on the precursor information of water inrush in karst tunnels: A true triaxial model test study. *Rock Mechanics and Rock Engineering* 52:373-384, DOI: [10.1007/s00603-018-1582-2](https://doi.org/10.1007/s00603-018-1582-2)
- Li YH, Yang S, Tang XJ, Ding YF, Zhang Q (2020b) Experimental investigation of the deformation and failure behavior of a tunnel excavated in mixed strata using transparent soft rock. *KSCSE Journal of Civil Engineering* 24(3):962-974, DOI: [10.1007/s12205-020-0072-8](https://doi.org/10.1007/s12205-020-0072-8)
- Li YY, Cui HQ, Zhang P, Wang DK, Wei JP (2020c) Three-dimensional visualization and quantitative characterization of coal fracture dynamic evolution under uniaxial and triaxial compression based on μ CT scanning. *Fuel* 262:116568, DOI: [10.1016/j.fuel.2019.116568](https://doi.org/10.1016/j.fuel.2019.116568)
- Li YZ, Zhou H, Liu HL, Ding XM, Zhang WG (2021b) Geotechnical properties of 3D-printed transparent granular soil. *Acta Geotechnica* 16:1789-1800, DOI: [10.1007/s11440-020-01111-7](https://doi.org/10.1007/s11440-020-01111-7)
- Lin W, Liu A, Mao W, Koseki J (2020) Acoustic emission behavior of granular soils with various ground conditions in drained triaxial compression tests. *Soils and Foundations* 60:929-943, DOI: [10.1016/j.sandf.2020.06.002](https://doi.org/10.1016/j.sandf.2020.06.002)
- Liu C, Tang XW, Wei HW, Wang PP, Zhao HH (2020) Model tests of jacked-pile penetration into sand using transparent soil and incremental particle image velocimetry. *KSCSE Journal of Civil Engineering* 24(4):1128-1145, DOI: [10.1007/s12205-020-1643-4](https://doi.org/10.1007/s12205-020-1643-4)
- Liu J, Liu XR, He C, Zhang KS, Wu ZS, Zeng B (2019) Analysis on the triaxial loading mechanical properties of sandstone under high stress and high hydraulic pressure. *Journal of Engineering Science and Technology Review* 12(4):113-121, DOI: [10.25103/jestr.124.14](https://doi.org/10.25103/jestr.124.14)
- Liu Q, Wang X, Song XD (2013) Study on test of the influence of moisture content on creep property of sandy slate coarse-grained soil. *Applied Mechanics and Materials* 405-408:1733-1738, DOI: [10.4028/www.scientific.net/AMM.405-408.1733](https://doi.org/10.4028/www.scientific.net/AMM.405-408.1733)
- Liu YR, Tang HM (2008) *Rock mechanics*. Chemical Industry Press, Beijing, China
- Lu N, Likos WJ (2004) *Unsaturated soil mechanics*. John Wiley & Sons, Hoboken, NJ, USA
- Lv ZX, Ji QQ, Ren WJ (2020) Experimental study and percolation analysis on seepage characteristics of fractured coal and sandstone based on real-time Micro-CT. *Geofluids* 2020:8832946, DOI: [10.1155/2020/8832946](https://doi.org/10.1155/2020/8832946)
- Mao HY, Liu SH, Shen CM, Wang LJ, Chu WT (2021) Development and application of a temperature-humidity controlled large triaxial apparatus for coarse granular materials. *Chinese Journal of Rock Mechanics and Engineering* 40:1-9, DOI: [10.13722/j.cnki.jrme.2020.0945](https://doi.org/10.13722/j.cnki.jrme.2020.0945) (in Chinese)
- Matsuoka H, Sun D, Kogane A, Fukuzawa N, Ichihara W (2002) Stress-strain behaviour of unsaturated soil in true triaxial tests. *Canadian Geotechnical Journal* 39:608-619, DOI: [10.1139/T02-031](https://doi.org/10.1139/T02-031)
- Meng FB, Huang J, Xiao P, Pang D, Jing HH (2020) Application of regional energy criterion in the prevention and control of coal mine rockburst. *IOP Conference Series: Earth and Environmental Science* 546:052017, DOI: [10.1088/1755-1315/546/5/052017](https://doi.org/10.1088/1755-1315/546/5/052017)
- Miyazaki K, Masui A, Sakamoto Y, Aoki K, Tenma N, Yamaguchi T (2011) Triaxial compressive properties of artificial methane-hydrate-bearing sediment. *Journal of Geophysical Research* 116:B06102, DOI: [10.1029/2010JB008049](https://doi.org/10.1029/2010JB008049)
- Nakashima K, Nakata Y, Hyodo M, Yoshimoto N, Hiraoka S, Kajiyama S (2021) Compressive characteristics of methane hydrate-bearing sands under isotropic consolidation. *Soils and Foundations* 61:506-519, DOI: [10.1016/j.sandf.2021.01.011](https://doi.org/10.1016/j.sandf.2021.01.011)
- Ng CWW, Zhou C (2014) Cyclic behaviour of an unsaturated silt at various suctions and temperatures. *Géotechnique* 64:709-720, DOI: [10.1680/geot.14.P015](https://doi.org/10.1680/geot.14.P015)
- Ng CWW, Zhan LT, Cui YJ (2002) A new simple system for measuring volume changes in unsaturated soils. *Canadian Geotechnical Journal* 39:757-764, DOI: [10.1139/T02-015](https://doi.org/10.1139/T02-015)
- Ni Q, Hird CC, Guymier I (2010) Physical modelling of pile penetration in clay using transparent soil and particle image velocimetry. *Géotechnique* 60(2):121-132, DOI: [10.1680/geot.8.P052](https://doi.org/10.1680/geot.8.P052)
- Nie RS, Sun BL, Leng WM, Li YF, Ruan B (2021) Resilient modulus of coarse-grained subgrade soil for heavy-haul railway: An experimental study. *Soil Dynamics and Earthquake Engineering* 150:106959, DOI: [10.1016/j.soildyn.2021.106959](https://doi.org/10.1016/j.soildyn.2021.106959)
- Ohtsu M, Isoda T, Tomoda Y (2007) Acoustic emission techniques standardized for concrete structures. *Journal of Acoustic Emission* 25:21-32
- Ohtsu M, Shigeishi M, Iwase H, Koyanagi W (1991) Determination of crack location, type and orientation in concrete structures by acoustic emission. *Magazine of Concrete Research* 43(155):127-134, DOI: [10.1680/mac.1991.43.155.127](https://doi.org/10.1680/mac.1991.43.155.127)
- Oldecop LA, Alonso EE (2001) A model for rockfill compressibility. *Géotechnique* 51:127-139, DOI: [10.1680/geot.2001.51.2.127](https://doi.org/10.1680/geot.2001.51.2.127)
- Oldecop LA, Alonso EE (2003) Suction effects on rockfill compressibility. *Géotechnique* 53:289-292, DOI: [10.1680/geot.2003.53.2.289](https://doi.org/10.1680/geot.2003.53.2.289)
- Oldecop LA, Alonso EE (2007) Theoretical investigation of the time-dependent behaviour of rockfill. *Géotechnique* 57:289-301, DOI: [10.1680/geot.2007.57.3.289](https://doi.org/10.1680/geot.2007.57.3.289)
- Otani J, Mukunoki T, Obara Y (2002) Characterization of failure in sand under triaxial compression using an industrial X-ray CT scanner. *International Journal of Physical Modelling in Geotechnics* 2(1):15-22, DOI: [10.1680/ijpmg.2002.020102](https://doi.org/10.1680/ijpmg.2002.020102)
- Pei F, Ji HG, Zhao JW, Geng JM (2020) Energy evolution and AE failure precursory characteristics of rocks with different rockburst proneness. *Advances in Civil Engineering* 2020:8877901, DOI: [10.1155/2020/8877901](https://doi.org/10.1155/2020/8877901)
- Priest JA, Druce M, Roberts J, Schultheiss P, Nakatsuka Y, Suzuki K (2015) PCATS Triaxial: A new geotechnical apparatus for characterizing pressure cores from the Nankai Trough, Japan. *Marine and Petroleum Geology* 66:460-470, DOI: [10.1016/j.marpetgeo.2014.12.005](https://doi.org/10.1016/j.marpetgeo.2014.12.005)
- Raghuandan ME, Sharma JS, Pradhan B (2015) A review on the effect of rubber membrane in triaxial tests. *Arabian Journal of Geosciences* 8:3195-3206, DOI: [10.1007/s12517-014-1420-0](https://doi.org/10.1007/s12517-014-1420-0)
- Rampino C, Mancuso C, Vinale F (1999) Laboratory testing on an unsaturated soil: Equipment, procedures, and first experimental results. *Canadian Geotechnical Journal* 36:1-12, DOI: [10.1139/t98-093](https://doi.org/10.1139/t98-093)
- Ranjith PG, Perera MSA (2011) A new triaxial apparatus to study the mechanical and fluid flow aspects of carbon dioxide sequestration in geological formations. *Fuel* 90:2751-2759, DOI: [10.1016/j.fuel.2011.04.004](https://doi.org/10.1016/j.fuel.2011.04.004)
- Rechenmacher AL (2006) Grain-scale processes governing shear band initiation and evolution in sands. *Journal of the Mechanics and Physics of Solids* 54:22-45, DOI: [10.1016/j.jmps.2005.08.009](https://doi.org/10.1016/j.jmps.2005.08.009)
- Rezaee R, Saeedi A, Clennell B (2012) Tight gas sands permeability estimation from mercury injection capillary pressure and nuclear magnetic resonance data. *Journal of Petroleum Science and Engineering* 88-89:92-99, DOI: [10.1016/j.petrol.2011.12.014](https://doi.org/10.1016/j.petrol.2011.12.014)
- Seol YK, Lei L, Choi JH, Jarvis K, Hill D (2019) Integration of triaxial testing and pore-scale visualization of methane hydrate bearing sediments. *Review of Scientific Instruments* 90:124504, DOI: [10.1063/1.5111111](https://doi.org/10.1063/1.5111111)

1.5125445

- Shao S, Wang Q, Luo A, Shao S (2017) True triaxial apparatus with rigid-flexible-flexible boundary and remolded loess testing. *Journal of Testing and Evaluation* 45(3):808-817, DOI: [10.1520/JTE20150177](https://doi.org/10.1520/JTE20150177)
- Shiotani T, Yuyama S, Li ZW, Ohtsu M (2001) Application of AE improved b-value to quantitative evaluation of fracture process in concrete materials. *Journal of Acoustic Emission* 19:118-133
- Siemens GA, Peters SB, Take WA (2013) Comparison of confined and unconfined infiltration in transparent porous media. *Water Resources Research* 49:851-863, DOI: [10.1002/wrcr.20101](https://doi.org/10.1002/wrcr.20101)
- Sohm J, Gabet T, Hornych P, Piau JM, Benedetto HD (2012) Creep tests on bituminous mixtures and modelling. *Road Materials and Pavement Design* 13:832-849, DOI: [10.1080/14680629.2012.735795](https://doi.org/10.1080/14680629.2012.735795)
- Song ZH, Hu YX, O'Loughlin C, Randolph MF (2009) Loss in anchor embedment during plate anchor keying in clay. *Journal of Geotechnical and Geoenvironmental Engineering* 135(10):1475-1485, DOI: [10.1061/\(ASCE\)GT.1943-5606.0000098](https://doi.org/10.1061/(ASCE)GT.1943-5606.0000098)
- Stanier SA, Hird CC, Black JA (2012) Enhancing accuracy and precision of transparent synthetic soil modelling. *International Journal of Physical Modelling in Geotechnics* 12(4):162-175, DOI: [10.1680/ijpmg.12.00005](https://doi.org/10.1680/ijpmg.12.00005)
- Su GS, Hu LH, Feng XT, Wang JH, Zhang XH (2016) True triaxial experimental study of rockburst process under low frequency cyclic disturbance load combined with static load. *Chinese Journal of Rock Mechanics and Engineering* 35(7):1309-1322, DOI: [10.13722/j.cnki.jrme.2015.1249](https://doi.org/10.13722/j.cnki.jrme.2015.1249) (in Chinese)
- Sultan N, Delage P, Cui YJ (2002) Temperature effects on the volume change behaviour of boom clay. *Engineering Geology* 64:135-145, DOI: [10.1016/S0013-7952\(01\)00143-0](https://doi.org/10.1016/S0013-7952(01)00143-0)
- Sun DA, Huang WX, Yao YP (2008) An experimental study of failure and softening in sand under three-dimensional stress condition. *Granular Matter* 10(3):187-195, DOI: [10.1007/s10035-008-0083-5](https://doi.org/10.1007/s10035-008-0083-5)
- Sun JZ, Liu JY (2014) Visualization of tunnelling-induced ground movement in transparent sand. *Tunnelling and Underground Space Technology* 40:236-240, DOI: [10.1016/j.tust.2013.10.009](https://doi.org/10.1016/j.tust.2013.10.009)
- Sun YT, Li GC, Yang S (2021) Rockburst Interpretation by a data-driven approach: A comparative study. *Mathematics* 9:2965, DOI: [10.3390/math922965](https://doi.org/10.3390/math922965)
- Uzun F, Korsunsky AM (2019) The height digital image correlation (hDIC) technique for the identification of triaxial surface deformations. *International Journal of Mechanical Sciences* 159:417-423, DOI: [10.1016/j.ijmecsci.2019.06.014](https://doi.org/10.1016/j.ijmecsci.2019.06.014)
- Voznesensky EA, Funikova VV, Babenko VA (2013) Deformability properties of model granular soils under true triaxial compression conditions. *Moscow University Geology Bulletin* 68(4):253-259, DOI: [10.3103/S014587521304008X](https://doi.org/10.3103/S014587521304008X)
- Wang DK, Zeng FC, Wei JP, Zhang HT, Wu Y, Wei Q (2021b) Quantitative analysis of fracture dynamic evolution in coal subjected to uniaxial and triaxial compression loads based on industrial CT and fractal theory. *Journal of Petroleum Science and Engineering* 196:108051, DOI: [10.1016/j.petrol.2020.108051](https://doi.org/10.1016/j.petrol.2020.108051)
- Wang JA, Park HD (2001) Comprehensive prediction of rockburst based on analysis of strain energy in rocks. *Tunnelling and Underground Space Technology* 16:49-57, DOI: [10.1016/S0886-7798\(01\)00030-X](https://doi.org/10.1016/S0886-7798(01)00030-X)
- Wang L, Sun X, Shen S, Wu P, Liu T, Liu WG, Zhao JF, Li YH (2021a) Undrained triaxial tests on water-saturated methane hydrate-bearing clayey-silty sediments of the South China Sea. *Canadian Geotechnical Journal* 58:351-366, DOI: [10.1139/cgj-2019-0711](https://doi.org/10.1139/cgj-2019-0711)
- Wang TT, Zhang T, Ranjith PG, Li YW, Song ZL, Wang S, Zhao WC (2020) A new approach to the evaluation of rock mass rupture and brittleness under triaxial stress condition. *Journal of Petroleum Science and Engineering* 184:106482, DOI: [10.1016/j.petrol.2019.106482](https://doi.org/10.1016/j.petrol.2019.106482)
- Wang Y (2018) The mechanical characteristics of rockfill materials under true triaxial stress conditions. PhD Thesis, Tsinghua University, Beijing, China
- Watanabe Y, Lenoir N, Otani J, Nakai T (2012) Displacement in sand under triaxial compression by tracking soil particles on X-ray CT data. *Soils and Foundations* 52(2):312-320, DOI: [10.1016/j.sandf.2012.02.008](https://doi.org/10.1016/j.sandf.2012.02.008)
- Wiebe B, Graham J, Tang GX, Dixon D (1998) Influence of pressure, saturation, and temperature on the behaviour of unsaturated sand-bentonite. *Canadian Geotechnical Journal* 35:194-205, DOI: [10.1139/t97-093](https://doi.org/10.1139/t97-093)
- Wood DM (1974) Some aspects of the mechanical behaviour of kaolin under truly triaxial conditions of stress and strain. PhD Thesis, University of Cambridge, Cambridge, UK
- Wulfsohn D, Adams BA, Fredlund DG (1998) Triaxial testing of unsaturated agricultural soils. *Journal of Agricultural Engineering Research* 69(4):317-330, DOI: [10.1006/jaer.1997.0251](https://doi.org/10.1006/jaer.1997.0251)
- Xiong YL, Liu GB, Zheng RY, Bao XH (2018) Study on dynamic undrained mechanical behavior of saturated soft clay considering temperature effect. *Soil Dynamics and Earthquake Engineering* 115:673-684, DOI: [10.1016/j.soildyn.2018.09.026](https://doi.org/10.1016/j.soildyn.2018.09.026)
- Xu J, Niu XL, Ma Q, Han QH (2021) Mechanical properties and damage analysis of rubber cement mortar mixed with ceramic waste aggregate based on acoustic emission monitoring technology. *Construction and Building Materials* 309:125084, DOI: [10.1016/j.conbuildmat.2021.125084](https://doi.org/10.1016/j.conbuildmat.2021.125084)
- Xu J, Shu SR, Han QH, Liu C (2018) Experimental research on bond behavior of reinforced recycled aggregate concrete based on the acoustic emission technique. *Construction and Building Materials* 191:1230-1241, DOI: [10.1016/j.conbuildmat.2018.10.054](https://doi.org/10.1016/j.conbuildmat.2018.10.054)
- Xu Y, Dai F (2018) Dynamic response and failure mechanism of brittle rocks under combined compression-shear loading experiments. *Rock Mechanics and Rock Engineering* 51:747-764, DOI: [10.1007/s00603-017-1364-2](https://doi.org/10.1007/s00603-017-1364-2)
- Yang WM, Wang MX, Zhou ZQ, Li LP, Yuan YC, Gao CL (2019) A true triaxial geomechanical model test apparatus for studying the precursory information of water inrush from impermeable rock mass failure. *Tunnelling and Underground Space Technology* 93:103078, DOI: [10.1016/j.tust.2019.103078](https://doi.org/10.1016/j.tust.2019.103078)
- Yang XR, Weng L, Hu ZX (2018) Damage evolution of rocks under triaxial compressions: An NMR investigation. *KSCSE Journal of Civil Engineering* 22(8):2856-2863, DOI: [10.1007/s12205-017-0766-8](https://doi.org/10.1007/s12205-017-0766-8)
- Yao XL, Qi JL, Yu F, Ma L (2013) A versatile triaxial apparatus for frozen soils. *Cold Regions Science and Technology* 92:48-54, DOI: [10.1016/j.coldregions.2013.04.001](https://doi.org/10.1016/j.coldregions.2013.04.001)
- Ye GL, Nishimura T, Zhang F (2015) Experimental study on shear and creep behaviour of green tuff at high temperatures. *International Journal of Rock Mechanics & Mining Sciences* 79:19-28, DOI: [10.1016/j.ijmms.2015.08.005](https://doi.org/10.1016/j.ijmms.2015.08.005)
- Yin JH, Cheng CM, Kumruzzaman M, Zhou WH (2010) New mixed boundary, true triaxial loading device for testing three-dimensional stress-strain-strength behaviour of geomaterials. *Canadian Geotechnical Journal* 47:1-15, DOI: [10.1139/T09-075](https://doi.org/10.1139/T09-075)
- Yin JH, Zhou WH, Kumruzzaman M, Cheng CM (2011) A rigid-flexible boundary true triaxial apparatus for testing soils in a three-dimensional stress state. *Geotechnical Testing Journal* 34(3):265-272, DOI: [10.1520/GTJ102886](https://doi.org/10.1520/GTJ102886)

- Yin LM, Guo WJ, Chen JT (2014a) Development of true triaxial rock test system of coupled stress-seepage and its application. *Chinese Journal of Rock Mechanics and Engineering* 33(supp.1):2820-2826, DOI: [10.13722/j.cnki.jrme.2014.s1.033](https://doi.org/10.13722/j.cnki.jrme.2014.s1.033) (in Chinese)
- Yin ZQ, Li XB, Jin JF, He XQ, Du K (2012) Failure characteristics of high stress rock induced by impact disturbance under confining pressure unloading. *Transactions of Nonferrous Metals Society of China* 22:175-184, DOI: [10.1016/S1003-6326\(11\)61158-8](https://doi.org/10.1016/S1003-6326(11)61158-8)
- Yin ZQ, Ma HF, Hu ZX, Zou Y (2014b) Effect of static-dynamic coupling loading on fracture toughness and failure characteristics in marble. *Journal of Engineering Science and Technology Review* 7(2):169-174, DOI: [10.25103/jestr.072.25](https://doi.org/10.25103/jestr.072.25)
- Yoneda J, Kida M, Konno Y, Jin Y, Morita S, Tenma N (2019) In situ mechanical properties of shallow gas hydrate deposits in the deep seabed. *Geophysical Research Letters* 46(24):14459-14468, DOI: [10.1029/2019GL084668](https://doi.org/10.1029/2019GL084668)
- Yue Y, Peng S, Liu Y, Xu J (2019) Investigation of acoustic emission response and fracture morphology of rock hydraulic fracturing under true triaxial stress. *Acta Geophysica* 67:1017-1024, DOI: [10.1007/s11600-019-00299-x](https://doi.org/10.1007/s11600-019-00299-x)
- Zhang BY, Zhang JH, Sun GL (2015) Deformation and shear strength of rockfill materials composed of soft siltstones subjected to stress, cyclical drying/wetting and temperature variations. *Engineering Geology* 190:87-97, DOI: [10.1016/j.enggeo.2015.03.006](https://doi.org/10.1016/j.enggeo.2015.03.006)
- Zhang BY, Zhang JH, Sun GL (2014a) Development of a soft-rock weathering test apparatus. *Experimental Techniques* 38:54-65, DOI: [10.1111/j.1747-1567.2011.00788.x](https://doi.org/10.1111/j.1747-1567.2011.00788.x)
- Zhang X, Mavroulidou M, Gunn MJ, Sutton J, Cabarkapa Z, Kichou Z (2014b) Application of a novel laser sensor volume measurement system to the triaxial testing of an unsaturated lime-treated soil. *Acta Geotechnica* 9:945-957, DOI: [10.1007/s11440-013-0254-3](https://doi.org/10.1007/s11440-013-0254-3)
- Zhang XH, Luo DS, Lu XB, Liu LL, Liu CL (2018) Mechanical properties of gas hydrate-bearing sediments during hydrate dissociation. *Acta Mechanica Sinica* 34:266-274, DOI: [10.1007/s10409-017-0699-y](https://doi.org/10.1007/s10409-017-0699-y)
- Zhang Y, Feng XT, Yang CX, Han Q, Wang ZF, Kong R (2021) Evaluation method of rock brittleness under true triaxial stress states based on pre-peak deformation characteristic and post-peak energy evolution. *Rock Mechanics and Rock Engineering* 54:1277-1291, DOI: [10.1007/s00603-020-02330-w](https://doi.org/10.1007/s00603-020-02330-w)
- Zhang YD, Buscarnera G (2018) Breakage mechanics for granular materials in surface-reactive environments. *Journal of the Mechanics and Physics of Solids* 112:89-108, DOI: [10.1016/j.jmps.2017.11.008](https://doi.org/10.1016/j.jmps.2017.11.008)
- Zhao Y, Wang CL, Ning L, Zhao HF, Bi J (2022) Pore and fracture development in coal under stress conditions based on nuclear magnetic resonance and fractal theory. *Fuel* 309:122112, DOI: [10.1016/j.fuel.2021.122112](https://doi.org/10.1016/j.fuel.2021.122112)
- Zheng F, Shao SJ, Wang J, Shao S (2020) Experimental study on the mechanical behaviour of natural loess based on suction-controlled true triaxial tests. *KSCE Journal of Civil Engineering* 24(8):2304-2321, DOI: [10.1007/s12205-020-1386-2](https://doi.org/10.1007/s12205-020-1386-2)
- Zheng F, Shao SJ, Wang YX, Shao S (2021) A new suction-controlled true triaxial apparatus for unsaturated soil testing. *Geotechnical Testing Journal* 44(4):833-850, DOI: [10.1520/GTJ20190015](https://doi.org/10.1520/GTJ20190015)
- Zhou CY, Lu YQ, Liu Z, Zhang LH (2019) An innovative acousto-optic-sensing-based triaxial testing system for rocks. *Rock Mechanics and Rock Engineering* 52:3305-3321, DOI: [10.1007/s00603-019-01764-1](https://doi.org/10.1007/s00603-019-01764-1)
- Zhou JZ, Wei CF, Wei HZ, Yang ZJ, Li LX, Li YL, Ding GR (2020a) Development and application of multi-functional triaxial test system for hydrate-bearing sediments. *Rock and Soil Mechanics* 41(1):342-352, DOI: [10.16285/j.rsm.2018.1896](https://doi.org/10.16285/j.rsm.2018.1896) (in Chinese)
- Zhou XX, Chi SC, Wang MH, Jia YF (2020b) Study on wetting deformation characteristics of coarse granular materials and its simulation in core-wall rockfill dams. *International Journal for Numerical and Analytical Methods in Geomechanics* 44(6):851-873, DOI: [10.1002/nag.3042](https://doi.org/10.1002/nag.3042)
- Zhu BZ, Fan JQ, Shi XY, Liu PF, Guo JQ (2021) Study on rockburst proneness of deep tunnel under different geo-stress conditions based on DEM. *Geotechnical and Geological Engineering* 13:3636, DOI: [10.1007/s10706-021-01969-8](https://doi.org/10.1007/s10706-021-01969-8)
- Zhu J, Deng JH, Huang YM, He ZL (2019) Influence of water on the fracture process of marble with acoustic emission monitoring. *KSCE Journal of Civil Engineering* 23(7):3239-3249, DOI: [10.1007/s12205-019-0172-5](https://doi.org/10.1007/s12205-019-0172-5)
- Zhu JH, Anderson SA (1998) Corrections for triaxial tests on undisturbed soils. *Journal of Testing and Evaluation* 26(3):277-284, DOI: [10.1520/JTE12002J](https://doi.org/10.1520/JTE12002J)
- Zhu WC, Li ZH, Zhu L, Tang CA (2010) Numerical simulation on rockburst of underground opening triggered by dynamic disturbance. *Tunnelling and Underground Space Technology* 25(5):587-599, DOI: [10.1016/j.tust.2010.04.004](https://doi.org/10.1016/j.tust.2010.04.004)